Neural Computing and Applications (2020) 32:6253–6282
https://doi.org/10.1007/s00521-019-04133-9

ORIGINAL ARTICLE

Novel computing paradigms for parameter estimation in power signal models

Ammara Mehmood[1] · Naveed Ishtiaq Chaudhary[2] · Aneela Zameer[3] · Muhammad Asif Zahoor Raja[4]

Received: 31 May 2018 / Accepted: 4 March 2019 / Published online: 12 March 2019

Abstract

The strength of evolutionary computational heuristic paradigms is exploited for parameter estimation of power signal modeling problems by incorporating differential evolution (DE), genetic algorithms (GAs) and pattern search (PS) methodologies. The objective function of power signal harmonics is constructed by utilizing the power of approximation theory in mean squared error sense. The stiff optimization task of signal harmonics is performed with heuristic solvers DE, GAs and PS that provide efficacy, fast convergence rate and avoid getting trapped in local minima. Statistics reveal that DE outperforms its counterparts in terms of accuracy, robustness and complexity measures.

Keywords Power signals · Parameter estimation · Differential evolution · Genetic algorithm · Pattern search algorithm · Evolutionary computing

1 Introduction

Electrical power supply systems are designed to ensure standard power provision to the consumers and the utilities. The ideal sinusoidal behavior of an AC power voltage or current signals distorts due to the excessive employment of power electronics devices, power converters, solid-state power switching devices, renewable power grid integration and nonlinear loads in electrical grid stations [1–5]. The distorted signals deteriorate the rated voltage and current, which badly affect the electrical equipment operations [6]. Due to these reasons, it is essential to monitor power quality of electrical networks by estimating the parameters for amplitudes, phases and frequencies to analyze the power signals. During the last few decades, researchers have made great effort toward estimating parameters of the signal models. Chen et al. provided several fast Fourier transform-based methods for parameter estimation [7]. Li studied least squares-based algorithms for power signals modeling [8]. Zhao et al. considered multifrequency identification technique for parameter estimation of various signal models [9]. Cao proposed hierarchical identification approach for estimation of signal frequency [10]. Ding et al. introduced recursive least squares and stochastic gradient-based parameter estimation techniques [11]. Adaptive filtering techniques were employed for the estimation of signal modeling parameters [12, 13]. Besides simple least square technique variations, i.e., bilinear recursive least square algorithm [14], forgetting factor [15] and variable constraint-based least mean square [16] were also investigated for estimation of signal components. These all are deterministic approaches, which are

✉ Aneela Zameer
aneelaz@pieas.edu.pk

Ammara Mehmood
ms_mehmud16@pieas.edu.pk; zad_mehmud@yahoo.com

Naveed Ishtiaq Chaudhary
Naveed.ishtiaq@iiu.edu.pk; naveedch835@gmail.com

Muhammad Asif Zahoor Raja
Muhammad.asif@ciit-attock.edu.pk;
rasifzahoor@yahoo.com

1 Department of Electrical Engineering, Pakistan Institute of Engineering and Applied Sciences, Nilore, Islamabad, Pakistan

2 Department of Electrical Engineering, International Islamic University, Islamabad, Pakistan

3 Department of Computer and Information Sciences, Pakistan Institute of Engineering and Applied Sciences, Nilore, Islamabad, Pakistan

4 Department of Electrical Engineering, COMSATS Institute of Information Technology, Attock, Pakistan

exhaustively applied for parameter identification of electrical power signals with their own perks and limitations, while stochastic solvers proficiency in nonlinear systems has not yet been widely exploited in harmonic estimation problems of various electrical networks.

The stochastic numerical optimization mechanisms based on evolutionary heuristics have been extensively applied for optimization of constrained and unconstrained problems in various domains [17–21]. Few notable applications of evolutionary computational technique include problems arising in computational fluid dynamics [22], electronic circuits [23], combustion theory [24], optimized power dispatch in electrical power system [25], optimal power flow solution [26], system identification [27], bioinformatics [28], controls [29], satellite systems design [30], magnetohydrodynamics [31], electrical machines [32], energy [33], plasma physics [34], astrophysics [35], atomic physics [36], signal processing [37], economic dispatch problem [38] and finance [39]. In the view of the above techniques, authors investigated the performance of new optimization techniques for stable and accurate parameter estimation of power signal modeling. In this research work, the strength of differential evolution (DE) optimization technique is employed for estimating fundamental signal model components by taking various noise variances and different model dynamics. The comparative performance of the proposed algorithm has also been carried out with renowned heuristic techniques based on genetic algorithms (GAs) and pattern search (PS) for different power signal models. The primary objectives of the proposed study are described as:

- Novel application of bioinspired heuristic computing through differential evolution is proposed for estimating fundamental components of power signal in the presence of noise with different variance levels.
- The objective function is formulated by exploiting the competency of approximation theory in mean squared error sense, and unknown adjustable variables of the system model are optimized with efficient global search tools based on differential evolution, genetic algorithms and pattern search method to draw constructive deductions.
- The efficacy, reliability and stability of the scheme are evaluated through comparison of true parameters of the power signal models with different degree of freedom based on amplitudes, frequencies, phases and their arbitrary combinations.
- Validation of the performance through statistic operators calculated for multiple executions of the algorithm in terms of mean absolute error (MAE), Nash–Sutcliffe efficiency (NSE) and Theil's inequality coefficient (TIC) along with their global versions.

Rest of the paper is organized as follows: The power signal model, objective function mathematical formulation, detailed description of designed methodology and optimization procedures are presented in Sect. 2. Discussion on the simulation results based on single run and multiple runs is provided in Sects. 3 and 4, respectively, in terms of tabular and graphical illustrations. Concluding remarks are listed in Sect. 5.

2 Design methodology

The proposed methodology for parameter estimation problem in power signal modeling consists of two parts; in the first step, system modeling of power signals is overviewed along with the development of the objective function in the mean squared error sense, while in the later stage, the optimization procedures for minimizing the error function are described. The detailed description of the designed scheme in the block processes is illustrated in Fig. 1.

2.1 Power signal modeling

The general form of electric alternating current signal can be described in terms of frequencies, phases and amplitudes as:

$$r(t) = \sum_{i=1}^{n} c_i \sin(\omega_i t + \varphi_i) = c_1 \sin(\omega_1 t + \varphi_1) + c_2 \sin(\omega_2 t + \varphi_2) + \cdots + c_n \sin(\omega_n t + \varphi_n), \tag{1}$$

where $\boldsymbol{c} = [c_1, c_2, \ldots, c_n]$ are the amplitudes of the peak deviation of the function from zero, the number of oscillations (cycles) that occur each second of time is $\boldsymbol{\omega} = [\omega_1, \omega_2, \ldots, \omega_n]$, the frequencies. $\boldsymbol{\varphi} = [\varphi_1, \varphi_2, \ldots, \varphi_n]$ are the phases (in radians) at $t = 0$ during oscillation. For all nonzero values of φ, the complete waveform emerges to be shifted in timescale by φ/ω seconds. A positive value of φ signifies an advance, while a negative value indicates a delay in the signal. Equation (1) appears in many report studies of engineering and applied sciences [40–42] and referenced therein.

In the experiment, the sampling time is $t_m = mh$, where h is sampling period. The observed data are shown as $\{t_k, r(t_k)\}$. Let $r_m = r(t_m)$ for implication; then, the discretized power signal based on sinusoidal function is given as:

$$r_m = \sum_{i=1}^{n} c_i \sin(\omega_i t_m + \varphi_i) = c_1 \sin(\omega_1 t_m + \varphi_1) + c_2 \sin(\omega_2 t_m + \varphi)_2 + \cdots + c_n \sin(\omega_n t_m + \varphi_n), \tag{2}$$

For $m = 1, 2, \ldots, M$

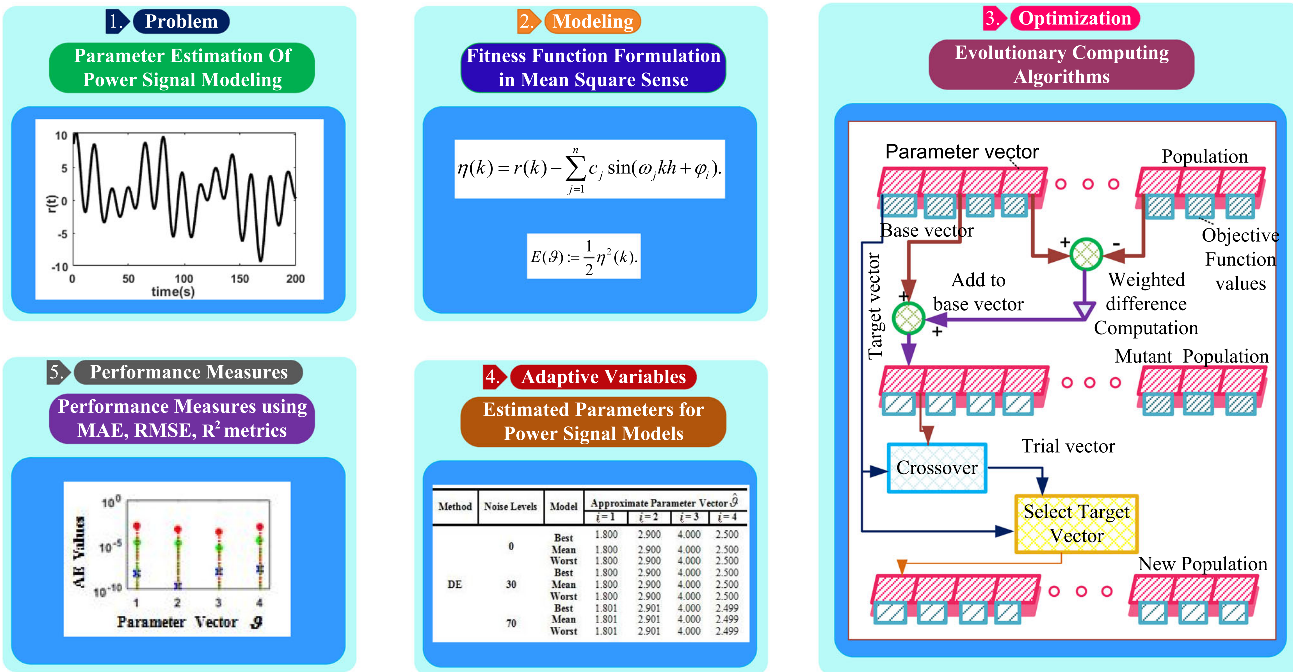

Fig. 1 Graphical abstract of the designed scheme

Standalone as well as the arbitrary combination of the parameters based on frequencies, phases and amplitudes of the sinusoidal-based signal model can be formulated for the estimation problems. The unknown parameters to be identified are given as:

$$\boldsymbol{\theta}_c = \boldsymbol{c} = [c_1, c_2, \ldots, c_n]^T \in \mathbb{R}^n \tag{3}$$

$$\boldsymbol{\theta}_\omega = \omega = [\omega_1, \omega_2, \ldots, \omega_n]^T \in \mathbb{R}^n \tag{4}$$

$$\boldsymbol{\theta}_\varphi = \varphi = [\varphi_1, \varphi_2, \ldots, \varphi_n]^T \in \mathbb{R}^n \tag{5}$$

$$\boldsymbol{\theta}_{c,\omega} = [\boldsymbol{c}, \boldsymbol{\omega}] = [c_1, c_2, \ldots, c_n, \omega_1, \omega_2, \ldots, \omega_n]^T \in \mathbb{R}^{2n} \tag{6}$$

$$\boldsymbol{\theta}_{c,\varphi} := [\boldsymbol{c}, \boldsymbol{\varphi}] = [c_1, c_2, \ldots, c_n, \varphi_1, \varphi_2, \ldots, \varphi_n]^T \in \mathbb{R}^{2n} \tag{7}$$

$$\boldsymbol{\theta}_{\omega,\varphi} := [\boldsymbol{\omega}, \boldsymbol{\varphi}] = [\omega_1, \omega_2, \ldots, \omega_n, \varphi_1, \varphi_2, \ldots, \varphi_n]^T \in \mathbb{R}^{2n} \tag{8}$$

$$\begin{aligned}\boldsymbol{\theta}_{c,\omega,\varphi} &:= [\boldsymbol{c},\ \boldsymbol{\omega},\ \boldsymbol{\varphi}] \\ &= [c_1, c_2, \ldots, c_n, \omega_1, \omega_2, \ldots, \omega_n, \varphi_1, \varphi_2, \ldots, \varphi_n]^T \\ &\in \mathbb{R}^{3n}\end{aligned} \tag{9}$$

The standalone parameter identification problems are based on Eqs. (3–5), while parametric Eqs. (6–9) represent the integrated parameter identification systems.

The fitness function for power signal modeling problem is formulated by exploiting the approximation theory in mean squared error sense as:

$$\varepsilon = \frac{1}{M}\sum_{m=1}^{M}\left(r_m - (\hat{r}_m + v_m)\right)^2 \tag{10}$$

$$\varepsilon = \frac{1}{M}\sum_{m=1}^{M}\left(\sum_{i=1}^{n} c_i \sin(\omega_i t_m + \varphi_i) - \sum_{i=1}^{n} \hat{c}_i \sin(\hat{\omega}_i t_m + \hat{\varphi}_i) - v_m\right)^2, \tag{11}$$

where $\boldsymbol{v} = [v_1, v_2, \ldots, v_m]$ is the noise signal with zero mean and constant variance, and $\hat{r}_m$ is the approximate signal with parameter vectors for amplitude, frequency and phase as:

$$\hat{\boldsymbol{\theta}}_c = \hat{\boldsymbol{c}} = [\hat{c}_1, \hat{c}_2, \ldots, \hat{c}_n]^T \in \mathbb{R}^n, \tag{12}$$

$$\hat{\boldsymbol{\theta}}_\omega = \hat{\omega} = [\hat{\omega}_1, \hat{\omega}_2, \ldots, \hat{\omega}_n]^T \in \mathbb{R}^n, \tag{13}$$

$$\hat{\boldsymbol{\theta}}_\varphi = \hat{\varphi} = [\hat{\varphi}_1, \hat{\varphi}_2, \ldots, \hat{\varphi}_n]^T \in \mathbb{R}^n, \tag{14}$$

accordingly, the variables $\hat{\boldsymbol{\theta}}_{c,\omega}$, $\hat{\boldsymbol{\theta}}_{c,\varphi}$, $\hat{\boldsymbol{\theta}}_{\omega,\varphi}$ and $\hat{\boldsymbol{\theta}}_{c,\omega,\varphi}$ of integrated parameter identification systems can be defined. Now the requirement is to optimize fitness function (10) such that ε approaches 0; then, the adaptive parameters $\hat{\boldsymbol{\theta}}_c$, $\hat{\boldsymbol{\theta}}_\omega$, $\hat{\boldsymbol{\theta}}_\varphi$, $\hat{\boldsymbol{\theta}}_{c,\omega}$, $\hat{\boldsymbol{\theta}}_{c,\varphi}$, $\hat{\boldsymbol{\theta}}_{\omega,\varphi}$ and $\hat{\boldsymbol{\theta}}_{c,\omega,\varphi}$ match with the true variables $\boldsymbol{\theta}_c$, $\boldsymbol{\theta}_\omega$, $\boldsymbol{\theta}_\varphi$, $\boldsymbol{\theta}_{c,\omega}$, $\boldsymbol{\theta}_{c,\varphi}$, $\boldsymbol{\theta}_{\omega,\varphi}$ and $\boldsymbol{\theta}_{c,\omega,\varphi}$ of the model.

2.2 Optimization procedure

The well-known global stochastic procedures DE, GAs and PS are used for estimation of signal model parameter vector $\boldsymbol{\theta}$ by optimizing objective function as described in Eq. (10), and brief introduction of these optimization solvers is given in this section.

DE is a stochastic optimization technique belonging to the class of evolutionary algorithms introduced by Storn and Price [43]. It is population-based search technique which mainly uses mutation as a search tool. Later the selection operation directs the search in the proximity of the feasible regions in the search space. Crossover and recombination operators are also used to search for better solution space. The generic flow graph with coherent designed steps of DE is shown in Fig. 2, while recent applications of DE are seen in solving different problems including text classification [44], reactive power management [45], hydrothermal energy scheduling problem [46], load dispatch involving wind power plant incorporating emission [47], nonlinear systems [48] and nanofluidics systems [49], while the renewed application of DE in diverse field can be seen latest review articles [50–53] and referenced therein. Genetic algorithms (GAs) belong to a family of evolutionary computational heuristics [54, 55]. Inspired by the theory of evolution, an optimal solution of a problem is determined through three basic genetic operators, i.e., mutation, selection and reproduction. The generic flow graph with essential procedural steps of GAs is presented in Fig. 2a. The global search efficacy of well-tuned, coherent structure and smooth implemented GAs can provide near-optimal solution for multiobjective,

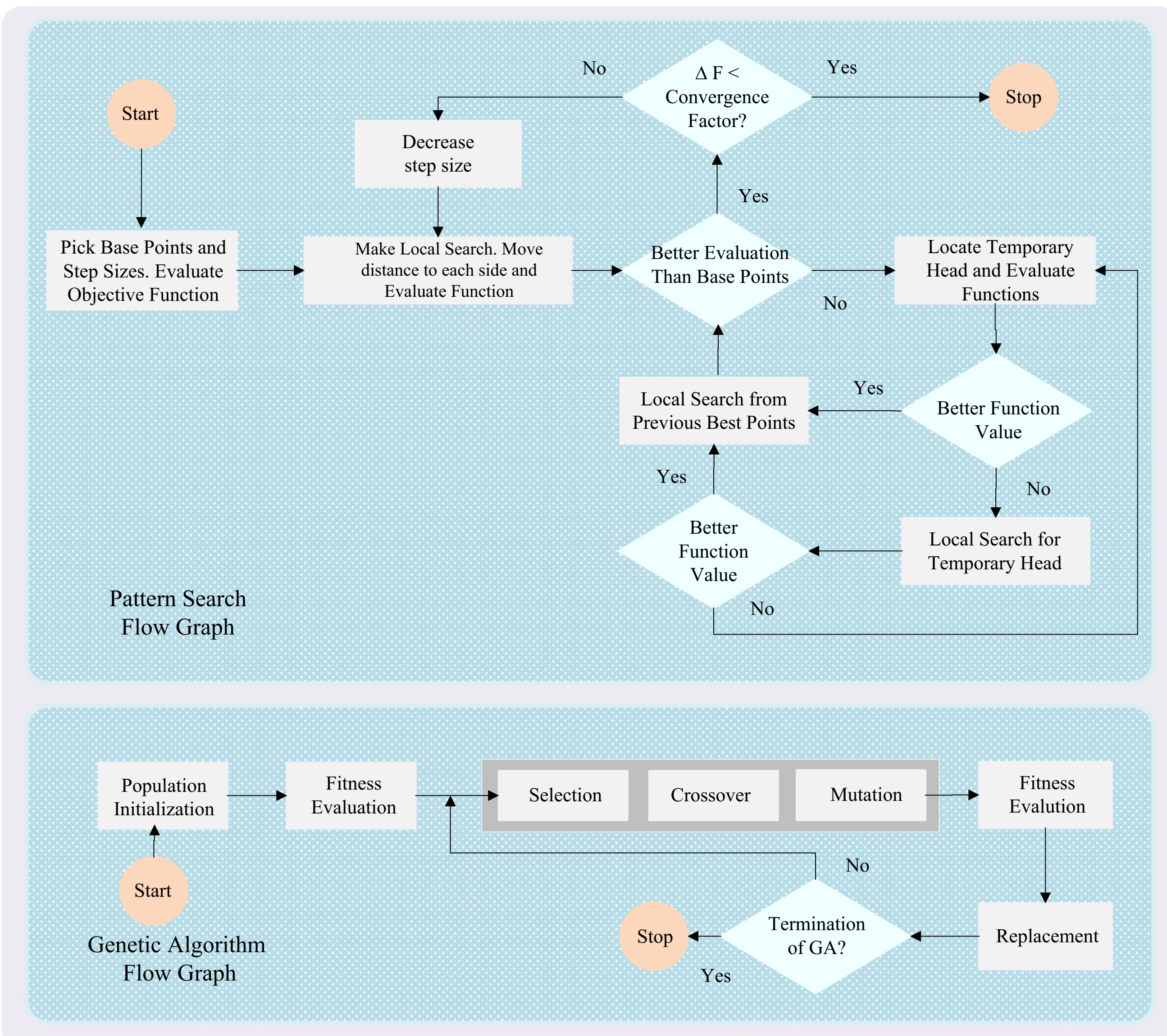

Fig. 2 Schematic workflow of PS and GAs

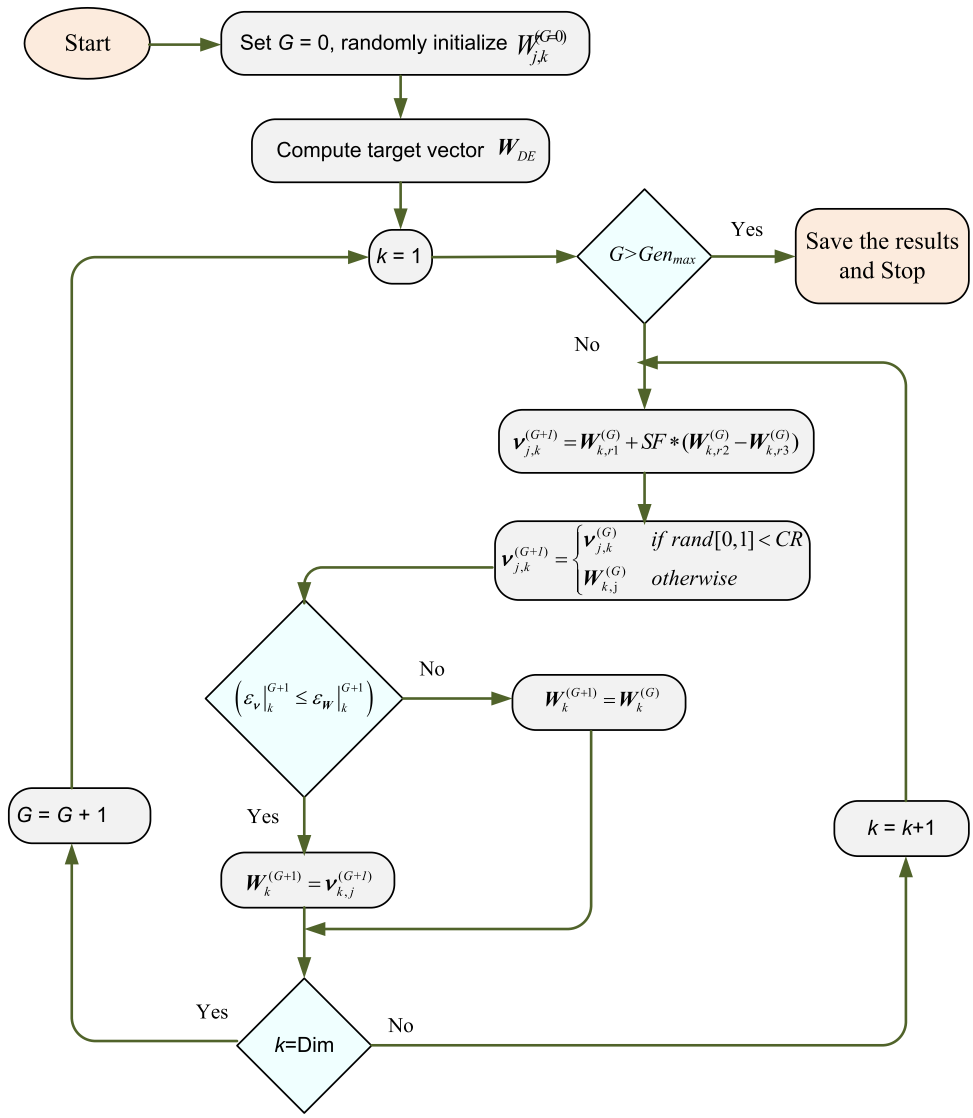

Fig. 3 Workflow diagram of DE for power signal modeling

multiconstraint, convex and nonconvex problems. This method was introduced by Holland [54, 55] and has several applications in science and engineering [56–61]. The PS is direct search optimization technique that does not require gradient information to search for minimal value of the cost function [62]. This method is exploited for nondifferentiable, stochastic and continuous functions. The pattern search algorithm computes a set of points known as a mesh around the initial/current point that tends to approach optimal value. When a current point is used to update a pattern, a mesh is created. The generic flow diagram with intermediate major steps of PS algorithm is illustrated in Fig. 2b [62], while the few recent application addresses with PS algorithm as can be seen in [63–66].

Efficiency of global optimizers DE, GAs and PS was the reason to utilize these optimization procedures for finding unknown parameters of signal model. The process flow graph of DE for signal model is presented in Fig. 3, while the detailed procedural steps are given in the form of pseudocode demonstrated in Table 1.

2.3 Performance indices

In this research study, performance evaluation of the designed methodology for parameter estimation of the power signal models is carried out using four performance indices, i.e., mean absolute error (MAE), root of mean squared error (RMSE), estimation error function and coefficient of determination (R^2). All these performance measures are briefly discussed in this section.

The performance measure MAE_c is described as:

Table 1 Pseudocode for DE algorithm for optimization of power signal modeling system

Part 1: DE

Input:

Chromosome or Individual ***W***

$$\boldsymbol{W} = \boldsymbol{\theta}_{c,\omega,\varphi} = [c_1, c_2, \ldots, c_n, \omega_1, \omega_2, \ldots, \omega_n, \varphi_1, \varphi_2, \ldots, \varphi_n]^T$$

Population of Chromosomes

$$\boldsymbol{P} = \begin{bmatrix} \boldsymbol{W}_1 \\ \boldsymbol{W}_2 \\ \vdots \\ \boldsymbol{W}_k \end{bmatrix} = \begin{bmatrix} c_{1,1}, c_{1,2}, \ldots, c_{1,n}, \omega_{1,1}, \omega_{1,2}, \ldots, \omega_{1,n}, \varphi_{1,1}, \varphi_{1,2}, \ldots, \varphi_{1,n} \\ c_{2,1}, c_{2,2}, \ldots, c_{2,n}, \omega_{2,1}, \omega_{2,2}, \ldots, \omega_{2,n}, \varphi_{2,1}, \varphi_{2,2}, \ldots, \varphi_{2,n} \\ \vdots \\ c_{k,1}, c_{k,2}, \ldots, c_{k,n}, \omega_{k,1}, \omega_{k,2}, \ldots, \omega_{k,n}, \varphi_{k,1}, \varphi_{k,2}, \ldots, \varphi_{k,n} \end{bmatrix},$$

Output:

Returned the best Weights of DE, $\boldsymbol{W}_{DE} = [\boldsymbol{\theta}_{c,\omega,\varphi}]_b$ with $\min \varepsilon$ as given in Eq. (10)

Begin DE

//Initialization of parameters
crossover probability (Pc)= 0.9,
scaling factor (SF)= 0.5,
population size (Pop)= 60, i.e., k in ***W***
dimensionality (Dim), i.e., n in ***W***
//Randomly generate *G*
for k= 1 to Pop ***do***
  For j= 1 to Dim ***do***

$$\boldsymbol{W}_{j,k}^{(G=0)} = \boldsymbol{W}_j^{min} + rand_j[0,1].(\boldsymbol{W}_j^{max} - \boldsymbol{W}_j^{min})$$

  end for
end for
//calculate ε
//For each *W* calculate ε as given in equation (10)
for k= 1 to Pop ***do***

$$\varepsilon\big|_k^{G+1}$$

end for
// Generate Test vectors using recombination operators
for k= 1 to Gen_{max} ***do***
  //Select three random vectors
  for l= 1 to *Pop* ***do***
    select randomly $r_1, r_2, r_3 \in [1, Pop], r_1 \neq r_2 \neq r_3 \neq k$
    //N each $\boldsymbol{W}$ goes through mutation, crossover operation
    //Generate random integer $jrand \in [1, Pop]$
    for j = 1 to D ***do***
      if*(rand[0,1]<CR or j==jrand)* ***then***

$$\boldsymbol{v}_{j,k}^{(G+l)} = \boldsymbol{W}_{k,r1}^{(G)} + SF * (\boldsymbol{W}_{k,r2}^{(G)} - \boldsymbol{W}_{k,r3}^{(G)})$$

      Else

$$\boldsymbol{v}_{j,k}^{(G+l)} = \boldsymbol{W}_{k,\mathrm{j}}^{(G)}$$

      end if
    end for
  end for
    //Selection Step
    if $\left(\varepsilon_{\boldsymbol{v}}\big|_k^{G+1} \leq \varepsilon_{\boldsymbol{W}}\big|_k^{G+1}\right)$ ***then***

$$\boldsymbol{W}_k^{(G+1)} = \boldsymbol{v}_{k,j}^{(G+l)}$$

    Else

$$\boldsymbol{W}_k^{(G+1)} = \boldsymbol{W}_k^{(G)}$$

    endif
  end for
End **DE**
//Accumulation step
Store $\boldsymbol{W}_{DE}$ with its ε, time, and generations for the each run of the DE.

End Part 1

Part 2: Statistics

To find optimal parameter of power signal model repeat the procedure for 100 independent executions to generate a dataset for efficient performance analysis of designed procedure.

End Part 2

$$\mathrm{MAE}_c = \frac{1}{n}\sum\nolimits_{i=1}^{n} \left|\boldsymbol{\theta}_{c,i} - \hat{\boldsymbol{\theta}}_{c,i}\right|. \tag{15}$$

where $\hat{\boldsymbol{\theta}}$ is an estimated weight vector of true vector $\boldsymbol{\theta}$. Similarly, the performance measure of $\mathrm{MAE}_{c,\omega}$, $\mathrm{MAE}_{c,\varphi}$, $\mathrm{MAE}_{\omega,\varphi}$, $\mathrm{MAE}_{c,\omega,\varphi}$ are formulated for $\hat{\boldsymbol{\theta}}_{c,\omega}$, $\hat{\boldsymbol{\theta}}_{c,\varphi}$, $\hat{\boldsymbol{\theta}}_{\omega,\varphi}$ and $\hat{\boldsymbol{\theta}}_{c,\omega,\varphi}$, respectively.

The RMSE is mathematically defined as:

$$\mathrm{RMSE}_c = \sqrt{\frac{1}{n}\sum_{i=1}^{n} (\boldsymbol{\theta}_{c,i} - \hat{\boldsymbol{\theta}}_{c,i})^2}, \tag{16}$$

Likewise, the root-mean-square errors for $\hat{\boldsymbol{\theta}}_{c,\omega}$, $\hat{\boldsymbol{\theta}}_{c,\varphi}$, $\hat{\boldsymbol{\theta}}_{\omega,\varphi}$ and $\hat{\boldsymbol{\theta}}_{c,\omega,\varphi}$ are also formulated mathematically.

Estimation error function δ is calculated as:

$$\delta = \frac{\left\|\hat{\boldsymbol{\theta}} - \boldsymbol{\theta}\right\|}{\|\boldsymbol{\theta}\|}, \tag{17}$$

where $\|\|$ represents the L^2 norm.

Coefficient of determination R_c^2 is determined as below:

$$R_c^2 = \left(\frac{\sum_{i=1}^{n} (\boldsymbol{\theta}_{c,i} - \bar{\boldsymbol{\theta}})(\hat{\boldsymbol{\theta}}_{c,i} - \boldsymbol{\theta})}{\sum_{i=1}^{n} \sqrt{(\boldsymbol{\theta}_{c,i} - \bar{\boldsymbol{\theta}})^2} \sum_{i=1}^{n} \sqrt{(\hat{\boldsymbol{\theta}}_{c,i} - \boldsymbol{\vartheta})^2}}\right)^2, \quad \mathit{for}\ \bar{\boldsymbol{\theta}} = \frac{1}{n}\sum_{i=1}^{n} \boldsymbol{\theta}_{c,i},\ \boldsymbol{\theta} = \frac{1}{n}\sum_{i=1}^{n} \hat{\boldsymbol{\theta}}_{c,i}. \tag{18}$$

The error in $R_c^2(\mathrm{ER}_c^2)$ is shown as:

$$\mathrm{ER}_c^2 = 1 - R_c^2. \tag{19}$$

Similarly, the performance indices $\mathrm{ER}^2_{c,\omega}$, $\mathrm{ER}^2_{c,\varphi}$, $\mathrm{ER}^2_{\omega,\varphi}$ and $\mathrm{ER}^2_{c,\omega,\varphi}$ are also defined for $\hat{\boldsymbol{\theta}}_{c,\omega}$, $\hat{\boldsymbol{\theta}}_{c,\varphi}$, $\hat{\boldsymbol{\theta}}_{\omega,\varphi}$ and $\hat{\boldsymbol{\theta}}_{c,\omega,\varphi}$, respectively.

The average fitness $\bar{\varepsilon}$ calculated from total number of runs R is illustrated as:

$$\bar{\varepsilon} = \begin{cases} \dfrac{1}{R}\displaystyle\sum_{r=1}^{R} \varepsilon_r \\ \dfrac{1}{R}\displaystyle\sum_{r=1}^{R} \left(\dfrac{1}{N}\displaystyle\sum_{i=1}^{N} \left(\left(\varphi^T(t_{c,i,r})\boldsymbol{\theta} + v(t_{c,i,r})\right) - \left(\varphi^T(t_{c,i,r})\hat{\boldsymbol{\theta}}\right)\right)^2\right). \end{cases} \tag{20}$$

Similarly, the global MAE ($G_{\mathrm{MAE}c}$) is mathematically evaluated as:

$$G_{\mathrm{MAE}c} = \frac{1}{R}\sum_{r=1}^{R} MAEc_r = \frac{1}{R}\sum_{r=1}^{R}\left(\sum_{i=1}^{n}\left|\boldsymbol{\theta}_{c,i} - \hat{\boldsymbol{\theta}}_{c,i}\right|\right), \tag{21}$$

where R represents the total number of independent executions, and one independent run is an algorithmic process with different random seeds. The global performance measures $G_{\mathrm{MAE}c,\omega}$, $G_{\mathrm{MAE}c,\varphi}$, $G_{\mathrm{MAE}\omega,\varphi}$ and $G_{\mathrm{MAE}c,\omega,\varphi}$ are also formulized for $\hat{\boldsymbol{\theta}}_{c,\omega}$, $\hat{\boldsymbol{\theta}}_{c,\varphi}$, $\hat{\boldsymbol{\theta}}_{\omega,\varphi}$ and $\hat{\boldsymbol{\theta}}_{c,\omega,\varphi}$, respectively.

Likewise, the global RMSE ($G_{\mathrm{RMSE}c}$) is formulated as,

$$G_{RMSEc} = \frac{1}{R}\sum_{r=1}^{R} RMSEc_r = \frac{1}{R}\sum_{r=1}^{R}\left(\sqrt{\frac{1}{n}\sum_{i=1}^{n}(\boldsymbol{\theta}_{c,i} - \hat{\boldsymbol{\theta}}_{c,i})^2}\right). \tag{22}$$

For $\hat{\boldsymbol{\theta}}_{c,\omega}$, $\hat{\boldsymbol{\theta}}_{c,\varphi}$, $\hat{\boldsymbol{\theta}}_{\omega,\varphi}$ and $\hat{\boldsymbol{\theta}}_{c,\omega,\varphi}$, the global performance operators are $G_{MAEc,\omega}$, $G_{MAEc,\varphi}$, $G_{MAE\omega,\varphi}$ and $G_{MAEc,\omega,\varphi}$, respectively.

Global ER_c^2 (G_{Rc}) is mathematically formalized as:

$$G_{Rc} = \begin{cases} \dfrac{1}{R}\displaystyle\sum_{r=1}^{R} \mathrm{ER}_c^2 \\ \dfrac{1}{R}\displaystyle\sum_{r=1}^{R}\left(\dfrac{\sum_{i=1}^{n}(\boldsymbol{\theta}_{c,i} - \bar{\boldsymbol{\theta}})(\hat{\boldsymbol{\theta}}_{c,i} - \boldsymbol{\vartheta})}{\sum_{i=1}^{n}\sqrt{(\boldsymbol{\theta}_{c,i} - \boldsymbol{\theta})^2}\sum_{i=1}^{n}\sqrt{(\hat{\boldsymbol{\theta}}_{c,i} - \boldsymbol{\vartheta})^2}}\right)^2. \end{cases} \tag{23}$$

The global performance operators $G_{Rc,\omega}$, $G_{Rc,\varphi}$, $G_{R\omega,\varphi}$ and $G_{Rc,\omega,\varphi}$ are also formulated for other four parameter vectors. In case of the perfect models, the standard values of these performance indices MAE, RMSE and ER^2 should be zero.

3 Simulation with discussion

The simulation results of numerical experimentation for five examples are presented for parameter estimation problem of power signal model with variation in optimization parameters as well as different signal-to-noise ratios using various heuristic computing techniques including DE and GAs and PS algorithms.

Example 1 *Power Signal with Unknown Amplitude*: In this example, the description of parameter estimation problem of power signal with unknown amplitude as parameter vector is considered as below:

$$\begin{aligned} r(t) &= c_1\sin(\omega_1 t + \varphi_1) + c_2\sin(\omega_2 t + \varphi_2) \\ &\quad + c_3\sin(\omega_3 t + \varphi_3) + c_4\sin(\omega_4 t + \varphi_4) \\ \boldsymbol{\theta}_c &= [c_1, c_2, c_3, c_4]^T \\ \boldsymbol{\theta}_c &= [1.8, 0.9, 4, 2.5]^{\mathrm{T}}. \end{aligned} \tag{24}$$

Example 2 *Power Signal with Unknown Amplitude and Frequency*: Here, an estimation problem of power signal with unknown amplitude and frequency is evaluated as:

$$\begin{aligned} r(t) &= c_1 \sin(\omega_1 t + \varphi_1) + c_2 \sin(\omega_2 t + \varphi_2) \\ &\quad + c_3 \sin(\omega_3 t + \varphi_3) \\ \boldsymbol{\theta}_{c,\omega} &= [c_1, c_2, c_3, \omega_1, \omega_2, \omega_3]^T \\ \boldsymbol{\theta}_{c,\omega} &= [0.8, 0.9, 0.4, 0.7, 0.5, 0.2]^T. \end{aligned} \tag{25}$$

Example 3 *Power Signal with Unknown Amplitude and Phase*: In this case study, parameter estimation of power signals having unknown amplitude and phase in the parameter vector is considered as follows:

$$\begin{aligned} r(t) &= c_1 \sin(\omega_1 t + \varphi_1) + c_2 \sin(\omega_2 t + \varphi_2) \\ &\quad + c_3 \sin(\omega_3 t + \varphi_3) \\ \boldsymbol{\theta}_{c,\varphi} &= [c_1, c_2, c_3, \varphi_1, \varphi_2, \varphi_3]^T \\ \boldsymbol{\theta}_{c,\varphi} &= [0.8, 0.6, 0.7, 0.6, 0.8, 0.76]^T. \end{aligned} \tag{26}$$

Example 4 *Power Signal with Unknown Frequency and Phase*: In this study, parameter estimation of power signal with unknown frequency and phase in the parameter vector is shown as follows:

$$\begin{aligned} r(t) &= c_1 \sin(\omega_1 t + \varphi_1) + c_2 \sin(\omega_2 t + \varphi_2) \\ &\quad + c_3 \sin(\omega_3 t + \varphi_3) \\ \boldsymbol{\theta}_{\omega,\varphi} &= [\omega_1, \omega_2, \omega_3, \varphi_1, \varphi_2, \varphi_3]^T \\ \boldsymbol{\theta}_{\omega,\varphi} &= [0.07, 0.1, 0.2, 0.95, 0.8, 0.76]^T. \end{aligned} \tag{27}$$

Example 5 *Power Signal with Unknown Amplitude, Frequency and Phase*: In this example, signal power parameter estimation model having unknown amplitude, frequency and phase in the parameter vector is described as follows:

$$\begin{aligned} r(t) &= c_1 \sin(\omega_1 t + \varphi_1) + c_2 \sin(\omega_2 t + \varphi_2) \\ &\quad + c_3 \sin(\omega_3 t + \varphi_3). \\ \boldsymbol{\theta}_{c,\omega,\varphi} &= [c_1, c_2, c_3, \omega_1, \omega_2, \omega_3, \varphi_1, \varphi_2, \varphi_3]^T \\ \boldsymbol{\theta}_{c,\omega,\varphi} &= [0.8, 0.9, 0.4, 0.95, 0.8, 0.76, 0.07, 0.5, 0.2]^T. \end{aligned} \tag{28}$$

Example 6 *Power Signal with Unknown Frequency and Phase*: In this example, signal parameter estimation model having unknown frequency and phase in the parameter vector is considered as follows:

$$\begin{aligned} r(t) &= c_1 \sin(\omega_1 t + \varphi_1) + c_2 \sin(\omega_2 t + \varphi_2) \\ &\quad + c_3 \sin(\omega_3 t + \varphi_3) \\ &\quad \ldots + c_4 \sin(\omega_4 t + \varphi_4) + c_5 \sin(\omega_5 t + \varphi_5). \\ \boldsymbol{\vartheta} &= [\omega_1, \omega_2, \omega_3, \omega_4, \omega_5, \varphi_1, \varphi_2, \varphi_3, \varphi_4, \varphi_5]^T \\ \boldsymbol{\vartheta} &= [0.07, 0.50, 0.20, 0.30, 0.10, 0.95, 0.80, 0.76, 0.60, 0.56]^T \end{aligned} \tag{29}$$

Example 7 *Power Signal with Unknown Amplitude, Frequency and Phase*: In this example, power signal parameter estimation model having unknown amplitude, frequency and phase in the parameter vector is given as follows:

$$\begin{aligned} r(t) &= c_1 \sin(\omega_1 t + \varphi_1) + c_2 \sin(\omega_2 t + \varphi_2) \\ &\quad + c_3 \sin(\omega_3 t + \varphi_3) + c_4 \sin(\omega_4 t + \varphi_4) \\ &\quad \ldots + c_5 \sin(\omega_5 t + \varphi_5) + c_6 \sin(\omega_6 t + \varphi_6) \\ &\quad + c_7 \sin(\omega_7 t + \varphi_7). \\ \boldsymbol{\vartheta} &= [c_1, c_2, c_3, c_4, c_5, c_6, c_7, \omega_1, \omega_2, \omega_3, \omega_4, \omega_5, \omega_6, \\ &\qquad \omega_7, \varphi_1, \varphi_2, \varphi_3, \varphi_4, \varphi_5, \varphi_6, \varphi_7]^T \\ \boldsymbol{\vartheta} &= [0.80, 0.07, 0.95, 0.90, 0.50, 0.80, 0.40, 0.20, \\ &\qquad 0.76, 0.10, 0.30, 0.60, \ldots 0.0020, 0.10, 0.56, \\ &\qquad 0.10, 0.10, 0.34, 0.10, 0.90, 0.24]^T \end{aligned} \tag{30}$$

In the present research study, five examples of power signal modeling are taken, the input signal $r(k)$ is a random signal sequence with zero mean and unit variance, and $v(t)$ is a noise signal with zero mean for different variance magnitudes. Three different noise levels are added to the signal which produce three noise scenarios, i.e., no noise scenario, 70-db and 30-db SNR levels, respectively, while the values of sampling period h and the data length L are set to 0.2 s and 2000 steps, respectively. The parameter estimation of the power signal model is performed with the designed methodologies based on DE, GAs and PS techniques, as discussed briefly in the previous section, while the parameter settings of all three algorithms for all seven examples are given in Table 2. However, fitness function (10) is formulated for M = 2000 for each case of all examples and is given as:

$$\varepsilon = \begin{cases} \dfrac{1}{2000}\displaystyle\sum_{m=1}^{2000} (r_m - (\hat{r}_m + v_m))^2 \\ \dfrac{1}{2000}\displaystyle\sum_{m=1}^{2000} \left(\sum_{i=1}^{n} c_i \sin(\omega_i t_m + \varphi_i) - \sum_{i=1}^{n} \hat{c}_i \sin(\hat{\omega}_i t_m + \hat{\varphi}_i) - v_m \right)^2, \end{cases} \tag{31}$$

For all five examples of power signal model, the optimization of objective function (31) is performed for three SNR levels employing optimization procedures based on DE, GAs and PS. The magnitudes of the performance metrics MAE, MWD, RMSE and ER^2 as defined in Eqs. (15) to (18) for each optimization technique are computed for 100 independent executions. The best run of the methodologies is revealed on the basis of the smallest magnitudes of all these performance indices

Table 2 Parameter settings for all examples of power signal modeling

Examples	Method	Parameters	Setting	Parameters	Setting
	DE	Generations	1000	Population size	150
1–5		Scaling factor	0.5	Unknowns	4/6/9
		Probability	0.99	Mutation	Random-best-2
	GA	Population creation	Constrained dependent	Population size	30 * num of variables
		Scaling function	Rank	Variables	4,6,9
		Selection function	Stochastic uniform	Generation	500
		Initial population	[− 1, 1]	Function tolerance	10^{-25}
		Crossover function	Scattered	Stall generation limit	250
		Mutation function	Adaptive feasible	Bounds (lower, upper)	(0,1)
		Elite count	10	Nonlinear constraint tolerance	10^{-25}
		Fitness limit	10^{-25}	Other	Defaults
	PS	Poll method	GPS positive base 2 N	Constraint tolerance	10^{-15}
		Polling order	Consecutive	Function tolerance	10^{-12}
		Max. iterations	3000	X-tolerance	10^{-15}
		Max. function evaluations	100,000	Mesh tolerance	10^{-15}
6–7	DE	Generations	5000	Population size	300
		Scaling factor	0.1	Unknowns	21/10
		Probability	0.5	Mutation	Random-best-2
	GA	Population creation	Constrained dependent	Population size	200
		Scaling function	Rank	Variables	21
		Selection function	Stochastic uniform	Generation	1000
		Initial population	[-0.1, 0.1]	Function tolerance	10^{-25}
		Crossover function	Scattered	Stall generation limit	250
		Mutation function	Adaptive feasible	Bounds (lower, upper)	(0,1)
		Elite count	5	Nonlinear constraint tolerance	10^{-25}
		Fitness limit	10^{-25}	Other	Defaults
	PS	Poll method	GPS positive base 2 N	Constraint tolerance	10^{-15}
		Polling order	Consecutive	Function tolerance	10^{-12}
		Max. iterations	3000	X-tolerance	10^{-15}
		Max. function evaluations	100,000	Mesh tolerance	10^{-15}

which are listed in Table 3 for all five examples of power signal modeling problems. Comparison of actual signal with the approximated signals is made and is plotted in Figs. 4, 5 and 6 for each designed methodology DE, GAs and PS, respectively. Absolute error (AE) values, i.e., deviation from the reference solution of power signals, are evaluated to further elaborate similarity level of the results with true solutions for all three SNR levels of each defined example.

The absolute error is computed for the run of the algorithm with minimum MAE value. The results of AE for all five examples of power signal model for each variation are shown graphically in Fig. 4a–f, for DE. Generally, the respective AE magnitudes lie around 10^{-10}, 10^{-06} and 10^{-03} for example 1, 10^{-10}, 10^{-06} and 10^{-04} for example 2, 10^{-10}, 10^{-06} and 10^{-04} for example 3, 10^{-10}, 10^{-05} and 10^{-03} in case of example 4 and 10^{-09}, 10^{-05} and 10^{-03} in case of example 5, for no noise scenario, 70-db SNR and 30-db SNR, respectively. Curves are also plotted in Fig. 4g–l comparing actual signal with the approximated signal. The computed solutions are found in good agreement with the actual numerical solutions. Comparison of MAE values for the first five examples is shown in subfigure, 4(m). Similar plots are also displayed for GAs, and PS is presented in Figs. 5 and 6, respectively.

The values of performance indices in terms of accuracy measures of fitness, MAE, RMSE and ER^2 are computed for the best execution of each algorithm, and results are listed in Table 4 for the first five examples, together with complexity measures based on time consumed, generations executed and function evaluated. It is clear that the values

Table 3 Best iteration of DE, GAs and PS algorithms based on different performance operators for each examples of power signal model

Example	Scheme	Operator	No noise		SNR = 70 db		SNR = 30 db	
			Best value	Iteration #	Best value	Iteration #	Best value	Iteration #
1.	DE	MAE	2.6E−10	55	5.90E−06	18	1.02E−03	37
		RMSE	3.2E−10	55	8.20E−06	64	1.18E−03	37
		R^2	2.8E−12	55	3.26E−10	64	6.79E−06	37
	GAs	MAE	1.6E−08	30	1.18E−05	9	7.46E−04	47
		RMSE	2.1E−08	77	1.48E−05	88	9.24E−04	71
		R^2	2.1E−15	77	1.07E−09	88	4.15E−06	71
	PS	MAE	2.8E−16	38	1.70E−05	54	3.25E−04	83
		RMSE	3.2E−16	38	2.12E−05	4	3.99E−04	10
		R^2	5.5E−15	38	2.18E−09	4	7.74E−07	10
2.	DE	MAE	1.9E−10	82	4.22E−06	92	2.34E−04	67
		RMSE	3.2E−10	82	6.73E−06	92	4.51E−04	13
		R^2	0.0E + 00	82	1.87E−10	92	8.36E−07	13
	GAs	MAE	5.3E−08	36	3.97E−06	13	7.94E−04	69
		RMSE	1.1E−07	96	7.37E−06	74	1.36E−03	69
		R^2	5.4E−14	96	2.23E−10	74	7.57E−06	69
	PS	MAE	7.7E−16	19	1.00E−01	68	5.97E−04	74
		RMSE	9.9E−16	19	1.29E−01	68	9.12E−04	74
		R^2	4.5E−16	19	6.88E−02	68	3.43E−06	74
3.	DE	MAE	1.9E−10	82	4.22E−06	92	2.34E−04	67
		RMSE	3.2E−10	82	6.73E−06	92	4.51E−04	13
		R^2	8.7E−10	82	1.87E−10	92	8.36E−07	13
	GAs	MAE	5.3E−08	36	3.97E−06	13	7.94E−04	69
		RMSE	1.1E−07	96	7.37E−06	74	1.36E−03	69
		R^2	5.4E−14	96	2.23E−10	74	7.57E−06	69
	PS	MAE	7.7E−16	19	1.00E−01	68	5.97E−04	74
		RMSE	9.9E−16	19	1.29E−01	68	9.12E−04	74
		R^2	3.4E−15	19	6.88E−02	68	3.43E−06	74
4.	DE	MAE	2.3E−10	65	2.46E−05	67	1.01E−03	78
		RMSE	3.4E−10	65	3.69E−05	67	1.81E−03	86
		R^2	1.9E−10	65	5.46E−09	67	1.31E−05	86
	GAs	MAE	7.2E−06	50	2.73E−05	17	4.74E−04	91
		RMSE	1.3E−05	50	4.50E−05	55	7.53E−04	91
		R^2	6.3E−10	50	8.12E−09	55	2.27E−06	91
	PS	MAE	2.3E−03	58	3.98E−03	93	1.79E−03	65
		RMSE	3.4E−03	58	5.66E−03	93	2.59E−03	65
		R^2	4.6E−05	58	1.28E−04	93	2.68E−05	65
5.	DE	MAE	2.0E−09	40	1.20E−05	57	1.15E−03	94
		RMSE	2.7E−09	40	2.09E−05	57	1.62E−03	94
		R^2	6.5E−09	40	1.81E−09	57	1.09E−05	94
	GAs	MAE	5.1E−04	74	1.18E−04	49	4.75E−04	46
		RMSE	8.6E−04	74	2.42E−04	49	6.88E−04	46
		R^2	3.1E−06	74	2.43E−07	49	1.97E−06	46
	PS	MAE	4.4E−02	18	7.54E−02	63	1.28E−01	34
		RMSE	8.7E−02	8	1.29E−01	63	1.97E−01	34
		R^2	3.2E−02	8	6.89E−02	63	1.62E−01	34

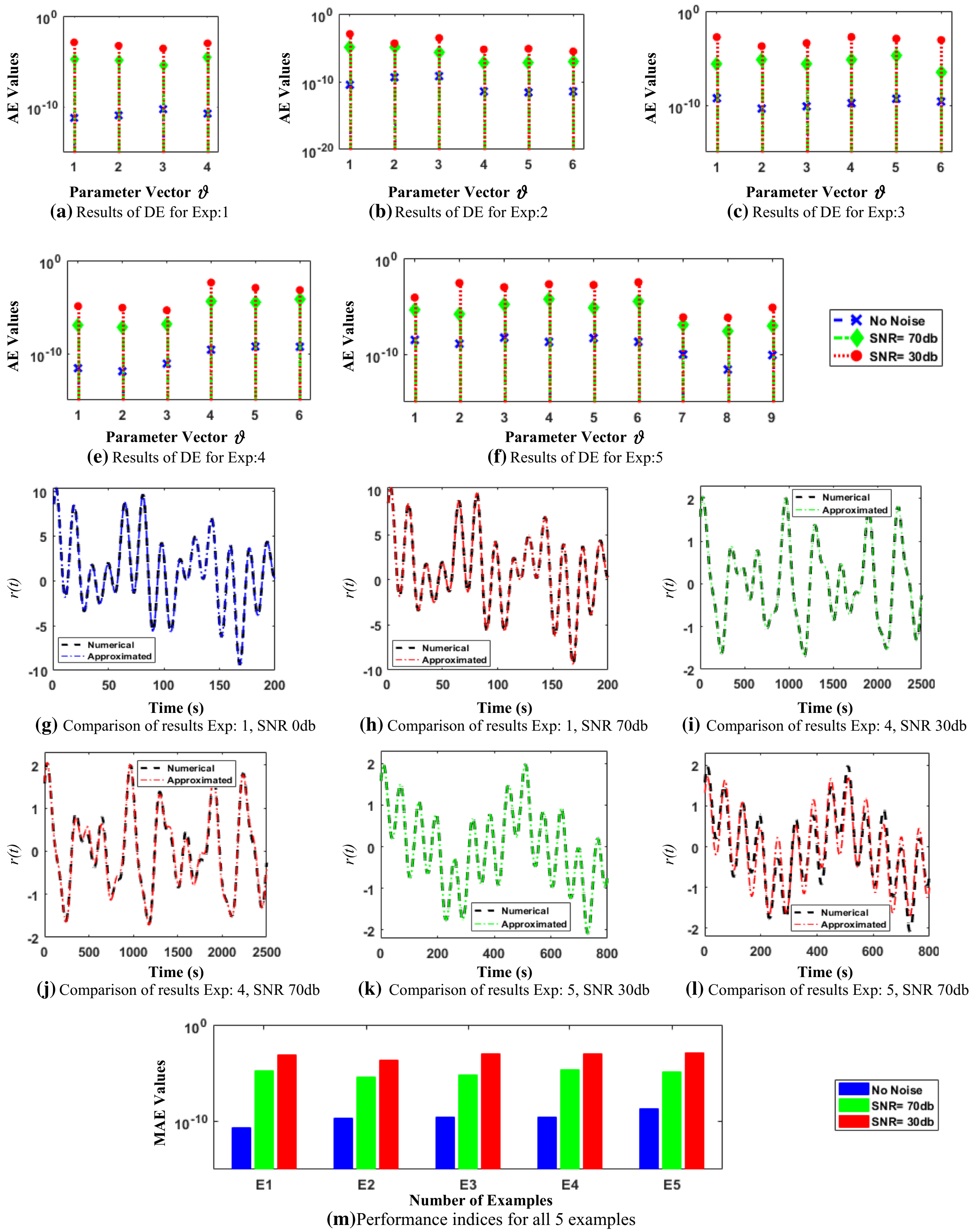

Fig. 4 Comparison results for DE in case of power signal models with different SNR levels

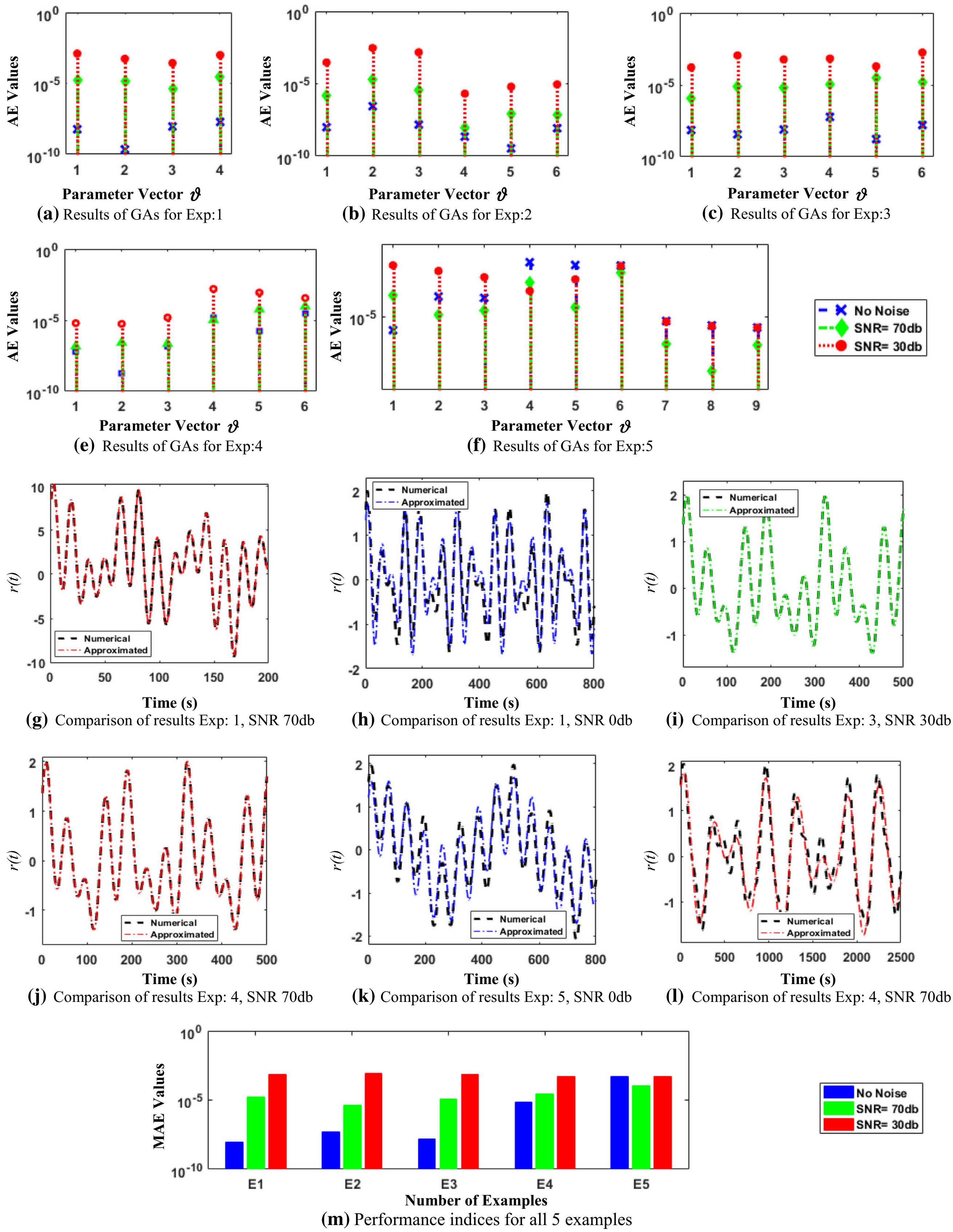

Fig. 5 Comparison results for GAs in case of power signal models with different SNR levels

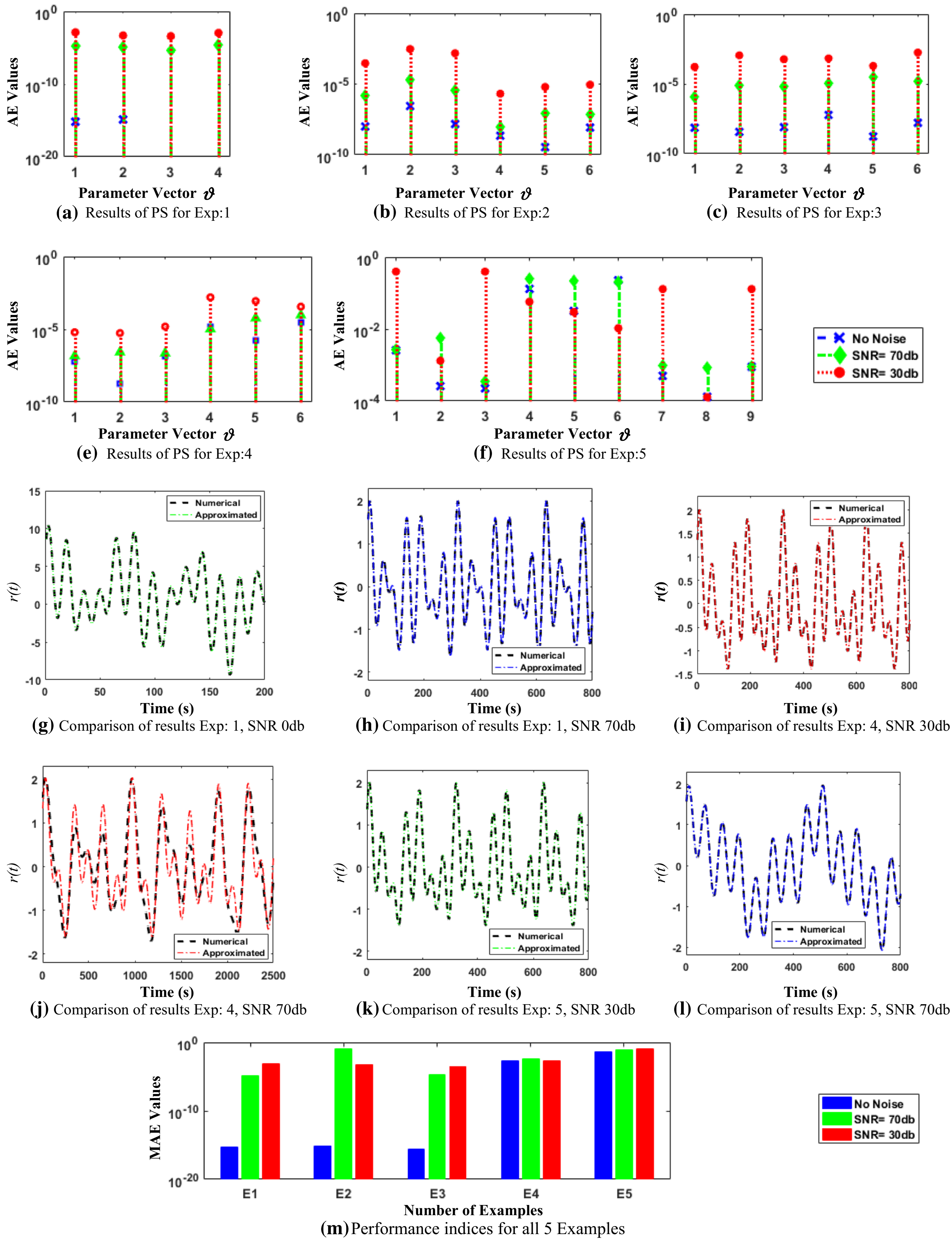

(a) Results of PS for Exp:1
(b) Results of PS for Exp:2
(c) Results of PS for Exp:3
(e) Results of PS for Exp:4
(f) Results of PS for Exp:5
(g) Comparison of results Exp: 1, SNR 0db
(h) Comparison of results Exp: 1, SNR 70db
(i) Comparison of results Exp: 4, SNR 30db
(j) Comparison of results Exp: 4, SNR 70db
(k) Comparison of results Exp: 5, SNR 30db
(l) Comparison of results Exp: 5, SNR 70db
(m) Performance indices for all 5 Examples

Fig. 6 Comparison results for PS in case of power signal models with different SNR levels

Table 4 Performance indices of accuracy and complexity for each algorithm for the first five examples of power signal model

Method	Example	Noise (db)	Accuracy					Complexity		
			ε	δ	MAE	RMSE	ER^2	Time	Generations	FCs
DE	1	0	3.7E−21	1.8E−11	4.3E−11	5.2E−11	3.3E−11	0.70	109	13,452
		70	5.9E−08	6.1E−06	1.6E−05	1.8E−05	6.2E−11	0.84	124	15,003
		30	6.4E−04	3.0E−04	7.7E−04	8.6E−04	1.5E−07	1.00	147	17,786
	2	0	2.4E−02	1.0E−00	4.6E−01	6.4E−01	1.7E−01	17.81	349	63,168
		70	1.2E−01	7.1E−01	3.6E−01	4.5E−01	8.2E−01	4.01	77	13,936
		30	6.4E−04	7.1E−04	2.3E−04	4.5E−04	8.4E−07	24.35	424	76,743
	3	0	6.5E−19	7.6E−10	3.9E−10	5.5E−10	0.0E−00	7.85	134	24,253
		70	6.0E−08	1.1E−05	5.9E−06	8.2E−06	3.3E−10	7.73	131	23,710
		30	6.3E−04	1.7E−03	1.0E−03	1.2E−03	6.8E−06	9.89	168	30,407
	4	0	1.0E−18	8.6E−03	3.4E−02	6.8E−01	1.9E−01	18.39	311	56,290
		70	6.5E−08	2.2E−01	2.3E−02	5.1E−01	1.0E−01	23.64	241	43,620
		30	6.5E−03	9.4E−01	3.0E−02	5.7E−01	1.3E−01	21.89	369	66,788
	5	0	3.7E−16	1.3E−00	8.7E−02	1.6E−00	1.0E−01	39.16	509	137,938
		70	6.7E−08	6.3E−00	1.3E−01	2.3E−00	2.2E−01	32.90	420	113,819
		30	1.5E−02	1.1E−01	2.8E−01	7.2E−00	2.1E−02	22.38	290	78589
GA	1	0	7.0E−16	7.7E−09	2.2E−08	2.3E−08	5.0E−09	31.23	500	120,240
		70	5.9E−08	6.0E−06	1.6E−05	1.8E−05	6.1E−11	33.78	500	120,240
		30	6.4E−04	3.0E−04	7.7E−04	8.6E−04	1.5E−07	32.45	500	120,240
	2	0	9.9E−05	5.3E−01	2.7E−01	3.4E−01	4.7E−01	33.31	500	120,240
		70	6.4E−08	1.3E−05	5.1E−06	8.2E−06	2.8E−10	33.39	500	120,240
		30	6.5E−04	2.2E−03	8.0E−04	1.4E−03	7.7E−06	41.15	500	120,240
	3	0	5.0E−15	7.7E−08	4.5E−08	5.5E−08	1.5E−14	38.25	500	120,240
		70	6.3E−08	2.2E−05	1.2E−05	1.5E−05	1.2E−09	35.09	500	120,240
		30	6.3E−04	1.3E−03	7.7E−04	9.5E−04	4.4E−06	38.66	500	120,240
	4	0	1.7E−10	2.1E−03	2.5E−05	3.7E−05	5.4E−09	32.89	500	120,240
		70	2.4E−07	2.3E−03	6.8E−04	9.7E−04	3.8E−06	36.23	500	120,240
		30	6.4E−04	2.3E−03	8.9E−04	1.4E−03	7.5E−06	36.78	500	120,240
	5	0	2.2E−05	3.2E−03	4.1E−03	7.3E−03	2.2E−04	37.45	500	120,240
		70	8.2E−06	3.3E−01	1.5E−01	2.2E−01	2.0E−01	42.65	500	120,240
		30	6.4E−04	4.4E−01	2.5E−01	2.9E−01	3.6E−01	43.86	500	120,240
PS	1	0	8.5E−31	2.6E−16	5.0E−16	7.4E−16	4.6E−11	0.08	158	1040
		70	5.9E−08	6.1E−06	1.6E−05	1.8E−05	6.3E−11	0.10	186	1229
		30	6.4E−04	3.1E−04	8.1E−04	9.0E−04	1.6E−07	0.15	290	1977
	2	0	3.7E−26	1.6E−15	7.7E−16	9.9E−16	0.0E−00	2.97	1000	8705
		70	1.9E−03	2.0E−01	1.0E−01	1.3E−01	6.9E−02	3.54	1182	10,079
		30	6.7E−04	1.4E−03	6.0E−04	9.1E−04	3.4E−06	3.25	922	7984
	3	0	7.7E−32	4.5E−16	2.8E−16	3.2E−16	0.0E−00	1.15	370	3635
		70	6.6E−08	3.0E−05	1.7E−05	2.1E−05	2.2E−09	1.76	552	5435
		30	6.1E−04	5.6E−04	3.2E−04	4.0E−04	7.7E−07	1.10	354	3490
	4	0	2.2E−06	2.0E−00	2.3E−03	3.4E−03	4.6E−05	4.22	1287	12,000
		70	6.0E−06	1.1E−00	4.0E−03	5.7E−03	1.3E−04	4.32	1275	12,000
		30	6.3E−04	4.3E−03	1.8E−03	2.6E−03	2.7E−05	3.90	1371	12,000
	5	0	1.5E−03	4.3E−01	4.4E−02	8.8E−02	3.2E−02	1.60	501	5836
		70	6.6E−03	6.8E−01	7.5E−02	1.3E−01	6.9E−02	1.54	501	5589
		30	3.2E−03	2.9E−01	1.3E−01	2.0E−01	1.6E−01	1.54	501	5666

Table 5 Performance indices of accuracy and complexity for each algorithm for examples 6 and 7 of power signal model

Method	Example	Noise (db)	Accuracy					Complexity		
			ε	δ	MAE	RMSE	ER^2	Time	Generations	FCs
DE	6	0	1.22E−07	5.95E−12	5.34E−06	2.16E−05	1.82E−07	34.51	5000	13,265
		70	1.06E−04	6.14E−08	4.08E−04	3.81E−04	2.94E−06	48.53	5000	22,511
		30	1.63E−02	6.33E−04	3.33E−02	7.16E−02	6.10E−04	55.75	5000	42,611
	7	0	1.19E−04	4.84E−07	1.06E−04	7.57E−05	3.15E−07	313.93	5000	153,785
		70	4.35E−03	1.96E−06	1.24E−03	1.42E−04	4.45E−04	354.81	5000	161,253
		30	3.37E−02	6.38E−04	9.31E−02	4.25E−03	3.22E−03	393.21	5000	173,225
GA	6	0	1.40E−06	7.34E−08	3.54E−06	7.28E−05	9.63E−07	280.46	1000	240,240
		70	1.52E−04	5.90E−06	4.66E−04	1.69E−02	4.32E−04	163.10	1000	240,240
		30	1.54E−02	6.38E−04	2.63E−02	1.59E−01	2.60E−03	188.28	1000	240,240
	7	0	6.41E−04	6.41E−06	7.43E−04	2.33E−04	3.45E−05	573.61	1000	450,655
		70	5.81E−03	8.75E−04	9.21E−03	7.45E−03	7.84E−04	392.23	1000	450,655
		30	6.75E−01	4.14E−03	8.76E−01	2.67E−01	6.56E−02	486.47	1000	450,655
PS	6	0	6.61E−02	5.94E−02	2.47E−02	8.28E−01	1.70E−02	2.16	657	6387
		70	6.14E−01	6.47E−02	5.14E−01	9.19E−01	5.38E−01	2.23	657	6397
		30	8.97E−00	5.92E−01	1.42E−01	6.60E−01	1.63E−01	2.65	657	6453
	7	0	4.78E−01	6.16E−01	1.28E−01	8.35E−01	3.42E−01	4.22	1500	24,050
		70	6.4E−00	6.3E−01	4.3E−00	8.4E−00	8.6E−00	4.32	1501	24,050
		30	1.0E−00	5.6E−01	2.1E−00	9.9E−00	2.7E−00	3.9	1500	24,050

of MAE are around 10^{-10} to 10^{-11}, 10^{-05} to 10^{-04} and 10^{-04} to 10^{-03} for no noise level, 70-db SNR and 30-db SNR, respectively, for DE in case of example 1, while for examples 2, 3, 4 and 5 the respective values lie 10^{-01} to 10^{-04}, 10^{-03} to 10^{-10}, 10^{-02} and 10^{-01} to 10^{-02}. Similarly, the values of performance indices along with complexity measures for examples 6 and 7 are listed in Table 5. The MAE magnitudes of DE and GAs are comparable, while PS algorithm depicts significantly low performance. It is observed from the figures that in example 3, among all designed procedures, GAs generate best results, while DE outperforms in example 5 on the basis of accuracy indicators, while in case of complexity measures, DE is found much more efficient than GAs as DE consumes less time, smaller number of generations and function calls than GAs. Very low values of these performance measures verify the stability of DE and GA schemes for estimating parameters of all examples of the power signal models.

It is important to note here that due to increased popularity of memetic computing methodologies, hybrid procedures based on combination of global and local search techniques are also suggested for power signal modeling identification problem. Recently, memetic computing-based methodologies are broadly used to find the candidate solution of the constrained/unconstrained and convex/nonconvex optimization problems, such as GAs aided with active-set method (GAs-ASM) [96], GAs integrated with sequential quadratic programming (GAs-SQP) [36, 61] and GAs hybrid with interior-point method (GAs-IPM) [37]. The hybrid schemes usually give better results than optimization techniques independently; therefore, hybridization of DE, GA and PS with local search mechanisms SQP, IPA and ASM for optimization of power signal models was also employed; however, no significant increase in the accuracy is achieved for all examples. Furthermore, local search techniques such as SQP, IPM and ASM were individually employed for estimation of components of power signal model and it was observed that due to nonconvex nature of the examples, these techniques failed to optimize their cost functions. For this reason, in the current article we restricted our analysis to three global search techniques based on DE, GAs and PS for identification of power signal models.

4 Statistics-based comparative analysis

In order to determine the stability and reliability of the proposed schemes, 100 independent runs were executed for each SNR level for all examples of power signal models

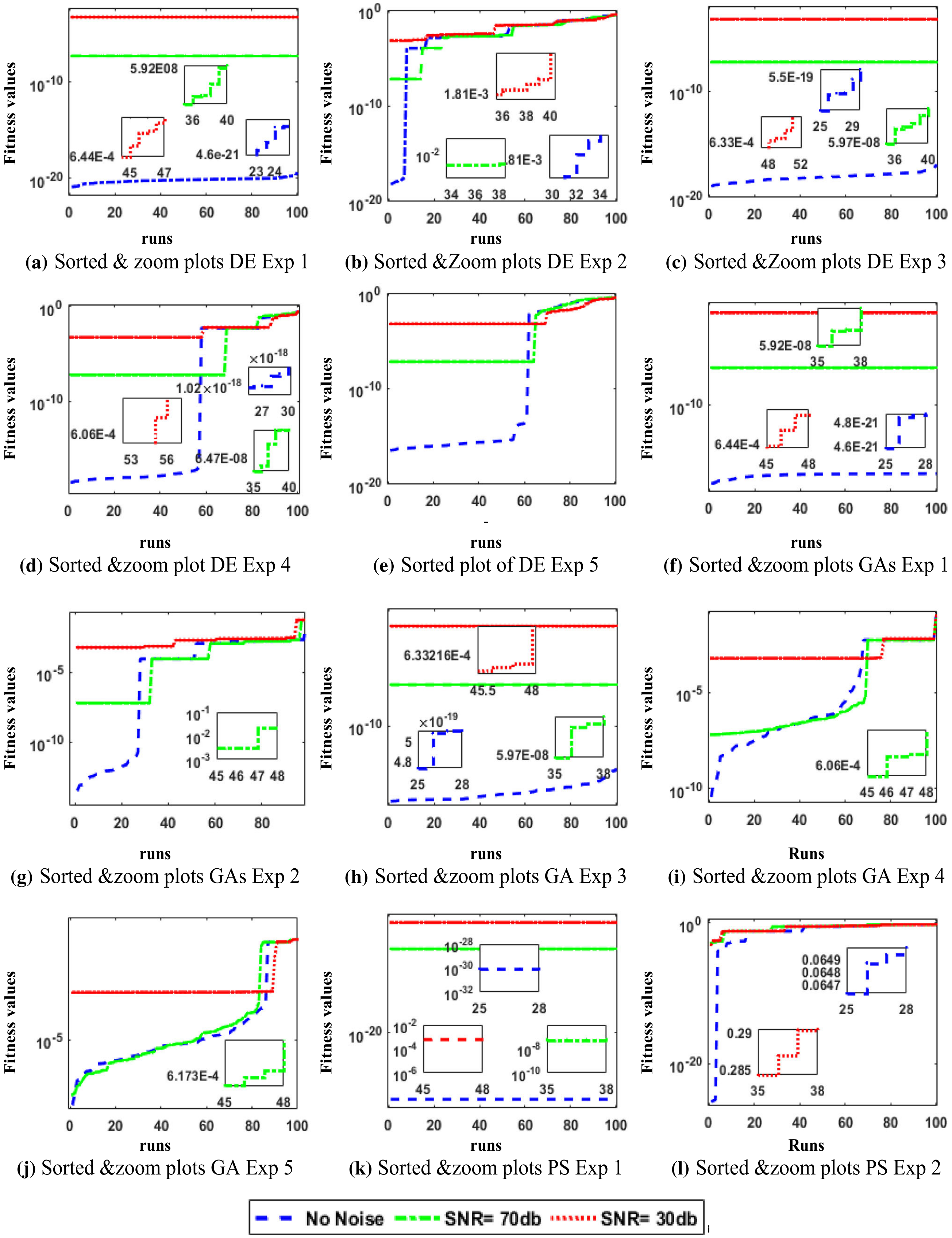

(a) Sorted & zoom plots DE Exp 1
(b) Sorted &Zoom plots DE Exp 2
(c) Sorted &Zoom plots DE Exp 3
(d) Sorted &zoom plot DE Exp 4
(e) Sorted plot of DE Exp 5
(f) Sorted &zoom plots GAs Exp 1
(g) Sorted &zoom plots GAs Exp 2
(h) Sorted &zoom plots GA Exp 3
(i) Sorted &zoom plots GA Exp 4
(j) Sorted &zoom plots GA Exp 5
(k) Sorted &zoom plots PS Exp 1
(l) Sorted &zoom plots PS Exp 2

Fig. 7 Plot of fitness for 100 runs of the algorithms in terms of sorted and zoomed illustrations

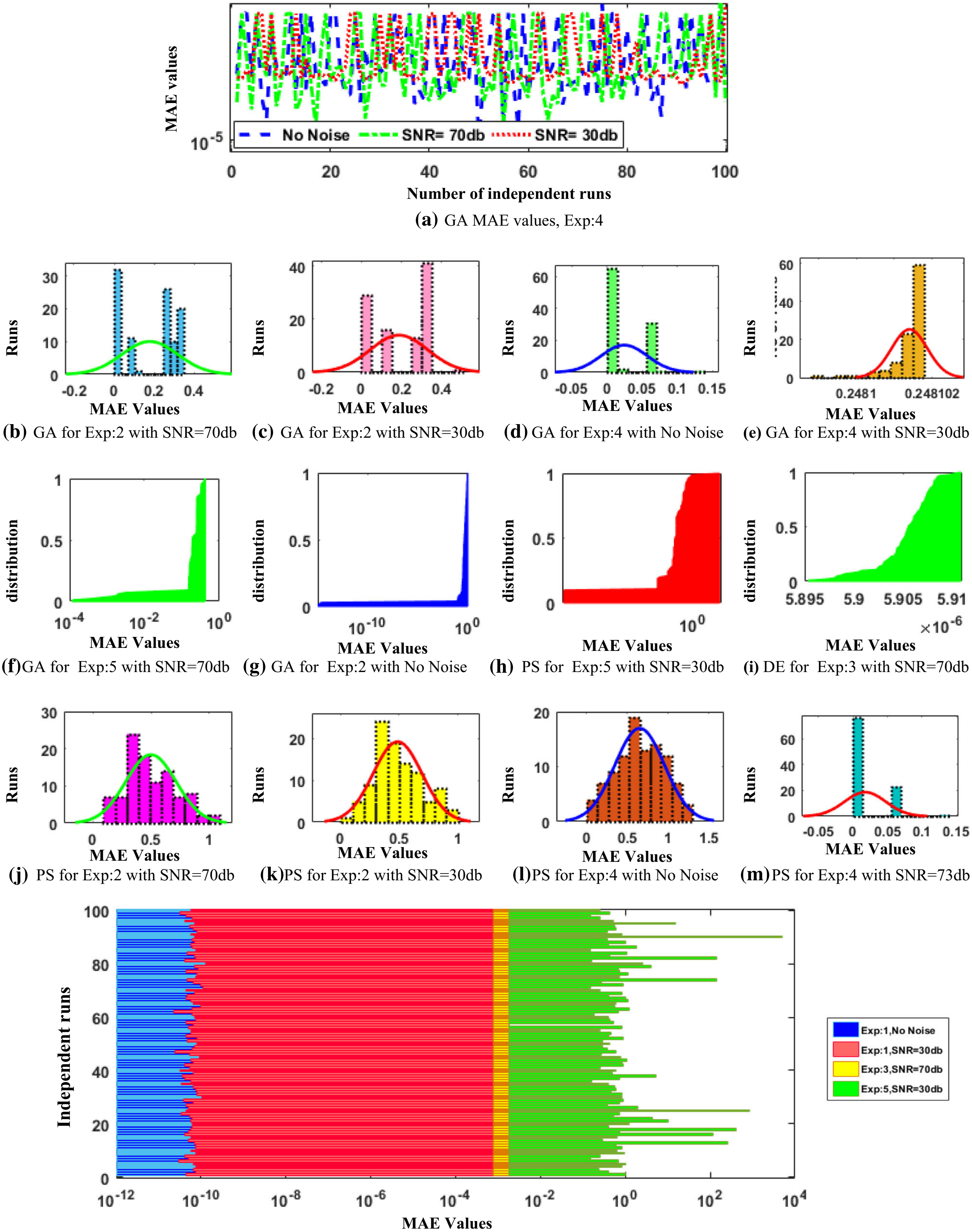

(a) GA MAE values, Exp:4

(b) GA for Exp:2 with SNR=70db **(c)** GA for Exp:2 with SNR=30db **(d)** GA for Exp:4 with No Noise **(e)** GA for Exp:4 with SNR=30db

(f) GA for Exp:5 with SNR=70db **(g)** GA for Exp:2 with No Noise **(h)** PS for Exp:5 with SNR=30db **(i)** DE for Exp:3 with SNR=70db

(j) PS for Exp:2 with SNR=70db **(k)** PS for Exp:2 with SNR=30db **(l)** PS for Exp:4 with No Noise **(m)** PS for Exp:4 with SNR=73db

(n) Result of DE in case of MAE magnitudes for Exp:1,SNR=0db, 30db, Exp:3,SNR=70db and Exp:5,SNR=30db

Fig. 8 Comparative study of DE, GA and PS based on MAEs for the first five examples (Exps) of power signal model

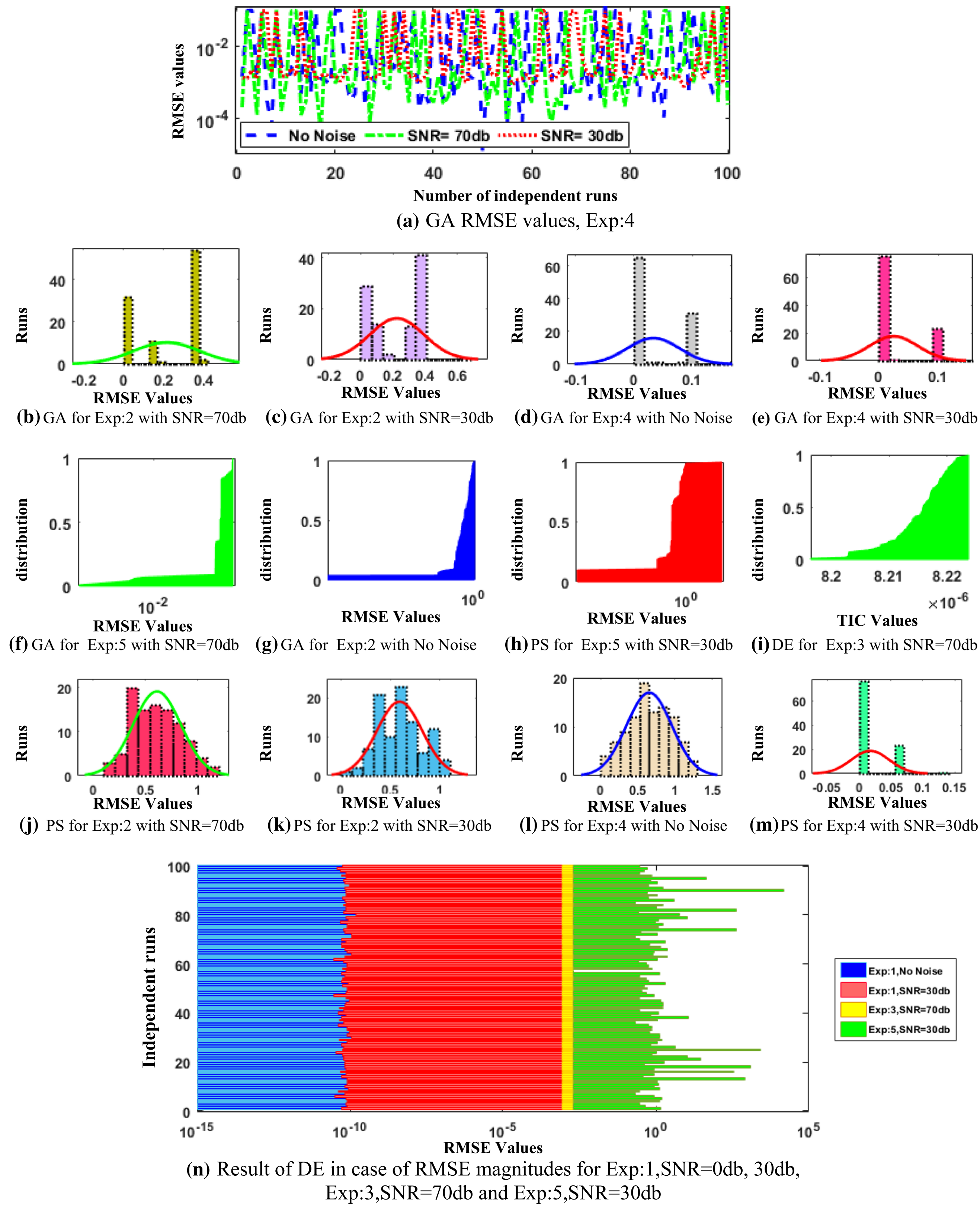

Fig. 9 Comparative study of DE, GA and PS based on RMSE magnitude for the first five examples (Exps) of power signal model

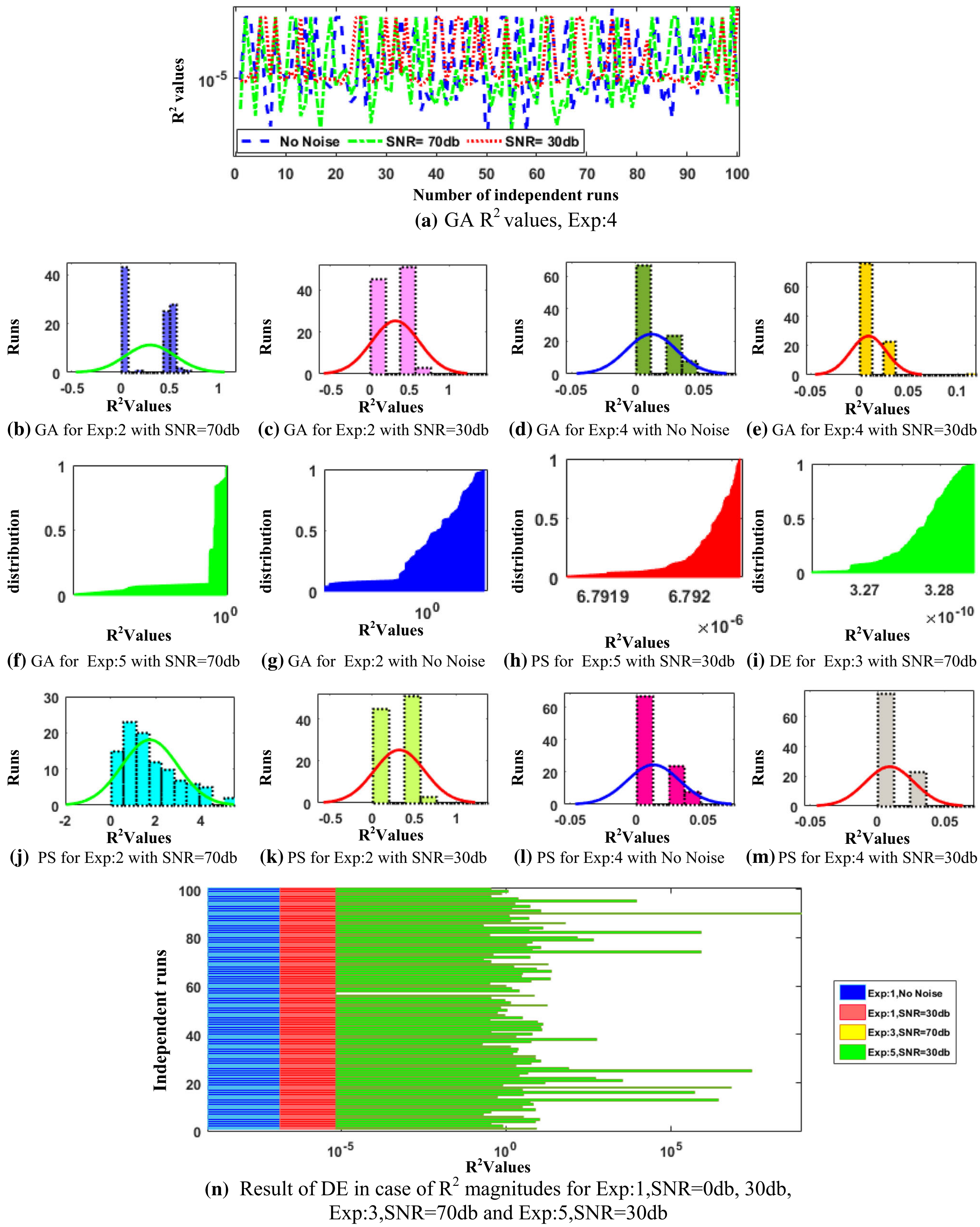

Fig. 10 Comparative study of DE, GA and PS based on R^2 magnitude for the first five examples (Exps) of power signal model

Table 6 Comparison of DE, GA and PS results through statistics for power signal model in case of all SNR levels for example 1

Method	Noise levels	Model	Approximate parameter vector $\hat{\theta}$			
			$i = 1$	$i = 2$	$i = 3$	$i = 4$
DE	0	Best	1.800	2.900	4.000	2.500
		Mean	1.800	2.900	4.000	2.500
		Worst	1.800	2.900	4.000	2.500
	70	Best	1.800	2.900	4.000	2.500
		Mean	1.800	2.900	4.000	2.500
		Worst	1.800	2.900	4.000	2.500
	30	Best	1.801	2.901	4.000	2.499
		Mean	1.801	2.901	4.000	2.499
		Worst	1.801	2.901	4.000	2.499
GA	0	Best	1.800	2.900	4.000	2.500
		Mean	1.800	2.900	4.000	2.500
		Worst	1.800	2.900	4.000	2.500
	70	Best	1.800	2.900	4.000	2.500
		Mean	1.800	2.900	4.000	2.500
		Worst	1.800	2.900	4.000	2.500
	30	Best	1.801	2.901	4.000	2.499
		Mean	1.801	2.901	4.000	2.499
		Worst	1.801	2.901	4.000	2.499
PS	0	Best	1.800	2.900	4.000	2.500
		Mean	1.800	2.900	4.000	2.500
		Worst	1.800	2.900	4.000	2.500
	70	Best	1.800	2.900	4.000	2.500
		Mean	1.800	2.900	4.000	2.500
		Worst	1.800	2.900	4.000	2.500
	30	Best	1.801	2.900	4.000	2.499
		Mean	1.801	2.900	4.000	2.499
		Worst	1.801	2.900	4.000	2.499
True values θ			1.8000	2.9000	4.000	2.900

and optimized results of fitness function values for several runs of each method are illustrated in Fig. 7. The graphs are given in sorted output and zoomed plots for better perception. The results based on performance metrics MAE, RMSE and ER^2 are presented in Figs. 8, 9, 10, respectively, for all designed approaches DE, GAs and PS. The results of GAs computed for each SNR level for the first five examples for power signal models are computed, and few plots are also presented in Figs. 7, 8 and 9a, for MAE, RMSE and ER^2, respectively. These plots are given in semi-logarithmic scale in order to decipher the results more clearly. The MAE values for power signal model of example 4 lie around 10^{-04} to 10^{-05}, 10^{-03} to 10^{-04} and 10^{-02} to 10^{-03} for no noise scenario, 70-db and 30-db SNRs, and similar trend is observed for performance measures of RMSE and ER^2, which shows the robustness of the schemes. For the analysis of consistency in precision, histogram studies are carried out and results based on MAE values for GAs are shown in Fig. 8b–e, and results based on PS are presented graphically in Fig. 8j–m. Empirical cumulative distribution function plots for all designed approaches are also plotted and are illustrated in Fig. 8f–i, while stacked bar plots for MAE values of DE for power signal modeling problem with few noise scenarios of different examples are also shown in Fig. 8n. Likewise, plots for RMSE and ER^2 are given in Figs. 9 and

Table 7 Comparison of DE, GA and PS results through statistics for power signal model in case of all SNR levels for example 2

Method	Noise levels	Model	Approximate parameter vector $\hat{\theta}$					
			$i = 1$	$i = 2$	$i = 3$	$i = 4$	$i = 5$	$i = 6$
DE	0	Best	0.800	0.900	0.400	0.700	0.500	0.200
		Mean	0.615	0.553	0.525	0.383	0.388	0.643
		Worst	0.875	0.432	0.550	0.500	0.706	0.192
	70	Best	0.800	0.900	0.400	0.700	0.500	0.200
		Mean	0.583	0.569	0.569	0.775	0.352	0.695
		Worst	0.133	0.955	0.802	0.678	0.500	0.700
	30	Best	0.799	0.900	0.400	0.700	0.500	0.200
		Mean	0.627	0.574	0.458	0.376	0.340	0.569
		Worst	0.870	0.548	0.424	0.500	0.695	0.171
GA	0	Best	0.800	0.400	0.900	0.700	0.200	0.500
		Mean	0.701	0.713	0.680	0.519	0.469	0.420
		Worst	0.907	0.150	0.788	0.500	0.604	0.701
	70	Best	0.800	0.900	0.400	0.700	0.500	0.200
		Mean	0.713	0.712	0.663	0.547	0.469	0.400
		Worst	0.907	0.150	0.788	0.500	0.604	0.701
	30	Best	0.800	0.897	0.399	0.700	0.500	0.200
		Mean	0.660	0.765	0.651	0.491	0.532	0.412
		Worst	0.790	0.049	0.905	0.700	1.800	0.500
PS	0	Best	0.797	0.397	0.074	0.700	0.200	0.553
		Mean	0.427	0.397	0.388	0.827	0.913	0.872
		Worst	0.027	0.037	0.132	2.000	1.995	1.405
	70	Best	0.894	0.800	0.061	0.500	0.700	1.395
		Mean	0.370	0.371	0.308	0.847	0.864	1.014
		Worst	0.018	0.037	0.127	1.956	1.995	1.905
	30	Best	0.115	0.050	0.089	0.099	0.992	0.292
		Mean	0.321	0.454	0.354	0.907	0.918	0.924
		Worst	0.036	0.081	0.117	0.010	1.998	1.706
True values θ			0.800	0.900	0.400	0.700	0.500	0.200

10, respectively. All these figures and plots verify that these designed approaches are capable of parameter estimation of power signal model, yet the DE and GAs results are comparatively better than PS. The algorithms DE and GAs are found parallel in terms of accuracy, while in example 5, DE outperforms GAs. The algorithm giving superior fitness value has corresponding better MAE, RMSE and ER^2 indices, which validate the accuracy through different performance measures.

Accuracy of the proposed methodology is further evaluated to observe the best, mean and the worst estimated parameter vector obtained on minimum error-based fitness, AEs in three noise scenarios for the first five examples of power signal model computed through 100 independent runs of DE, GAs and PS approaches. Outcomes of statistical measures for the three approaches are presented in Tables 6, 7, 8, 9, 10 for three SNR levels of examples 1–5 with their actual parameters, respectively. The parameter estimation performance of DE, GAs and PS algorithms is dependent on the noise variance, such as for larger SNR level, performance of the designed procedures reduces. Furthermore, by increasing the length of the parameter vector of the power signal model, a small decrease in the accuracy of the proposed algorithms is observed which is understandable as with more degrees of freedom, the optimization problem gets stiffer.

In order to draw reliable inference on the precision, the global performance metrics $\bar{E}$, G_{MAE}, G_{RMSE} and G_{ER^2}

Table 8 Comparison of DE, GA and PS results through statistics for power signal model in case of all SNR levels for example 3

Method	Noise levels	Model	Approximate parameter vector $\hat{\theta}$					
			$i = 1$	$i = 2$	$i = 3$	$i = 4$	$i = 5$	$i = 6$
DE	0	Best	0.800	0.600	0.700	0.600	0.800	0.760
		Mean	0.800	0.600	0.700	0.600	0.800	0.760
		Worst	0.800	0.600	0.700	0.600	0.800	0.760
	70	Best	0.800	0.600	0.700	0.600	0.800	0.760
		Mean	0.800	0.600	0.700	0.600	0.800	0.760
		Worst	0.800	0.600	0.700	0.600	0.800	0.760
	30	Best	0.798	0.600	0.700	0.598	0.801	0.759
		Mean	0.798	0.600	0.700	0.598	0.801	0.759
		Worst	0.798	0.600	0.700	0.598	0.801	0.759
GA	0	Best	0.800	0.600	0.700	0.600	0.800	0.760
		Mean	0.800	0.600	0.700	0.600	0.800	0.760
		Worst	0.800	0.600	0.700	0.600	0.800	0.760
	70	Best	0.800	0.600	0.700	0.600	0.800	0.760
		Mean	0.800	0.600	0.700	0.600	0.800	0.760
		Worst	0.800	0.600	0.700	0.600	0.800	0.760
	30	Best	0.800	0.601	0.701	0.599	0.800	0.758
		Mean	0.800	0.601	0.701	0.599	0.800	0.758
		Worst	0.800	0.601	0.701	0.599	0.800	0.758
PS	0	Best	0.800	0.600	0.700	0.600	0.800	0.760
		Mean	0.800	0.600	0.700	0.600	0.800	0.760
		Worst	0.800	0.600	0.700	0.600	0.800	0.760
	70	Best	0.800	0.600	0.700	0.600	0.800	0.760
		Mean	0.800	0.600	0.700	0.600	0.800	0.760
		Worst	0.800	0.600	0.700	0.600	0.800	0.760
	30	Best	0.800	0.599	0.700	0.600	0.800	0.759
		Mean	0.800	0.599	0.700	0.600	0.800	0.759
		Worst	0.800	0.599	0.700	0.600	0.800	0.759
True values θ			0.800	0.600	0.700	0.600	0.800	0.760

magnitudes are computed based on multiple executions of DE, GAs and PS as described in Eqs. (11)–(14), respectively. Result is tabulated in Table 11 for the first five examples of the power signal systems for each SNR level. On the basis of fitness, the accuracy level for global operators is found in the order of 10^{-02} to 10^{-21} for DE, 10^{-04} to 10^{-16} for GAs and 10^{-01} to 10^{-16} for PS in all examples of power signal models, whereas the range of performance indices of MAE, RMSE and ER^2 is approximately 10^{-01} to 10^{-10} for DE and GAs and 10^{-01} to 10^{-16} for PS methods. The attained global performance metrics have values almost close to their ideals, which verify the correctness of the DE- and GAs-based methodologies for each example of power signal model.

The performance of the proposed algorithms is further evaluated using ANOVA test for power signal modeling problem. The results are generated for the first five examples of the power signal models, and results are presented only for complex scenarios, i.e., example 4 with 70-dB SNR and example 5 with 30-dB SNR, in Tables 12 and 13, respectively. While considering the assumption of homogeneity of variances, the null hypothesis of homogeneous variances at the significance level 0.05 cannot be rejected, as the respective probability values attained for AE in case of DE, GAs and PS are 0.895, 0.810 and 0.821 for example 4, while in case of example 5, the respective probability values are 0.897, 0.695 and 0.107. This indicates that the expected values in the three groups do not have any strong evidence of

Table 9 Comparison of DE, GA and PS results through statistics for power signal model in case of all SNR levels for example 4

Method	Noise levels	Model	Approximate parameter vector $\hat{\theta}$					
			$i = 1$	$i = 2$	$i = 3$	$i = 4$	$i = 5$	$i = 6$
DE	0	Best	0.070	0.100	0.200	0.950	0.800	0.760
		Mean	0.150	0.066	0.467	1.211	0.997	0.760
		Worst	0.100	0.070	0.200	0.823	2.156	0.812
	70	Best	0.070	0.100	0.200	0.950	0.800	0.760
		Mean	0.045	0.061	0.126	1.113	1.017	0.739
		Worst	0.070	0.100	0.200	0.950	0.800	0.640
	30	Best	0.070	0.100	0.200	0.954	0.801	0.759
		Mean	0.214	0.071	0.746	1.090	0.982	0.746
		Worst	0.070	0.100	0.200	2.187	0.801	0.625
GA	0	Best	0.070	0.100	0.200	0.950	0.800	0.760
		Mean	0.081	0.090	0.199	0.905	0.859	0.752
		Worst	0.200	0.100	0.070	0.599	0.704	0.854
	70	Best	0.070	0.100	0.200	0.950	0.800	0.760
		Mean	0.079	0.091	0.199	0.907	0.857	0.762
		Worst	0.099	0.070	0.100	0.504	0.972	1.931
	30	Best	0.070	0.100	0.200	0.952	0.801	0.760
		Mean	0.078	0.093	0.199	0.919	0.843	0.751
		Worst	0.200	0.100	0.070	0.596	0.697	0.845
PS	0	Best	0.070	0.100	0.200	0.954	0.804	0.766
		Mean	0.906	0.749	0.841	0.976	0.898	0.754
		Worst	1.923	1.898	1.901	1.170	0.000	2.000
	70	Best	0.070	0.100	0.200	0.943	0.807	0.751
		Mean	0.823	0.761	0.831	0.867	0.834	0.922
		Worst	1.988	1.984	1.974	2.000	0.000	0.000
	30	Best	0.070	0.100	0.200	0.947	0.796	0.755
		Mean	0.812	0.706	0.774	0.960	0.888	0.890
		Worst	1.762	1.597	1.600	0.000	0.000	2.000
True values θ			0.070	0.100	0.2	0.950	0.800	0.760

variation in the response variable of uniformity. Thus, it is quite significant that all means are equal. Additionally, it is seen from the values of confidence interval that DE and GAs provide better results than PS, while DE performs comparatively better than GAs. The same trend prevails with similar inferences for rest of the cases on the basis of ANOVA test.

Computational complexity for all three algorithms, DE, GAs and PS, is analyzed through calculating the time, each algorithm consumed for hundred independent runs, iteration executed and objective functions evaluated, for optimization of the first five examples of power signal model for different noise levels, and results are tabulated in Table 14. Average time expended, generation executed and functions evaluated are around 16 $\pm$ 14, 750 $\pm$ 550, 51,200 $\pm$ 48,100 for DE, 37 $\pm$ 5, 500, 120,240 for GAs, 2.5 $\pm$ 1.1, 750 $\pm$ 550 and 5827 $\pm$ 4100 for PS, respectively. It is observed that with the increase in the length of parameter vector of power signal model, the complexity of DE and PS increases significantly, whereas GAs-based extensive global search does not show such behavior. In general, GAs complexity is much more than that of DE and PS, while its accuracy is found parallel with DE. All the simulations are performed in this research work on HP ProDesk 400 G3, Processor core i7, 3.4 GHz, RAM 8 GB, using MATLAB 2016a running in Windows 8.1 professional environment.

5 Concluding remarks

Strength of nature-inspired heuristics based on DE, GAs and PS is efficiently exploited in power signal modeling through estimating the necessary components of the power signal. Comparative studies reveal that all the three

Table 10 Comparison of DE, GA and PS results through statistics for power signal model in case of all SNR levels for example 5

Method	Noise levels	Model	Approximate parameter vector $\hat{\theta}$								
			$i = 1$	$i = 2$	$i = 3$	$i = 4$	$i = 5$	$i = 6$	$i = 7$	$i = 8$	$i = 9$
DE	0	Best	0.800	0.900	0.400	0.950	0.800	0.760	0.070	0.500	0.200
		Mean	0.503	0.414	0.447	0.103	3.862	0.605	0.191	0.299	0.172
		Worst	0.900	0.800	0.400	0.800	0.950	0.670	0.500	0.070	0.200
	70	Best	0.800	0.900	0.400	0.950	0.800	0.760	0.070	0.500	0.200
		Mean	0.401	0.504	0.351	0.130	0.810	0.870	0.167	0.496	0.196
		Worst	0.900	0.400	0.800	0.800	0.820	0.830	0.500	0.200	0.070
	30	Best	0.800	0.897	0.399	0.952	0.802	0.763	0.070	0.500	0.200
		Mean	0.504	0.409	0.349	1.010	0.900	0.550	0.216	0.186	0.193
		Worst	0.897	0.800	0.399	0.802	0.952	0.640	0.500	0.070	0.200
GA	0	Best	0.900	0.400	0.800	0.800	0.754	0.951	0.500	0.200	0.070
		Mean	0.659	0.712	0.694	0.847	0.889	0.899	0.301	0.228	0.295
		Worst	0.164	0.804	0.899	2.000	0.949	0.802	0.601	0.070	0.500
	70	Best	0.801	0.900	0.399	0.948	0.808	0.754	0.070	0.500	0.200
		Mean	0.665	0.644	0.747	0.850	0.951	0.849	0.263	0.270	0.299
		Worst	0.165	0.803	0.899	2.000	0.956	0.787	0.601	0.070	0.500
	30	Best	0.799	0.399	0.901	0.945	0.764	0.801	0.070	0.200	0.500
		Mean	0.634	0.731	0.705	0.871	0.869	0.855	0.262	0.280	0.268
		Worst	0.161	0.802	0.899	2.000	0.963	0.789	0.601	0.070	0.500
PS	0	Best	0.063	0.122	0.148	0.200	1.308	0.000	0.124	0.664	0.357
		Mean	0.407	0.354	0.367	0.976	0.997	0.950	0.618	0.731	0.603
		Worst	0.052	0.226	0.071	1.012	1.999	1.999	1.904	1.072	1.347
	70	Best	0.143	0.091	0.083	0.495	0.091	1.453	1.059	1.945	1.245
		Mean	0.323	0.343	0.445	0.891	0.963	1.004	0.782	0.679	0.617
		Worst	0.127	0.232	0.069	1.776	1.996	2.000	1.505	1.072	1.346
	30	Best	0.828	0.035	0.214	0.953	1.041	1.999	0.070	0.006	1.501
		Mean	0.368	0.371	0.351	1.031	0.943	0.879	0.685	0.698	0.801
		Worst	0.127	0.088	0.106	2.000	0.000	0.000	1.348	1.623	1.923
True values θ			0.80	0.90	0.800	0.900	0.400	0.950	0.800	0.760	0.070

proposed algorithms are effective; however, estimation ability reduced for the model with more degrees of freedom for each approach, but the estimation of DE outperforms its counterparts GAs and PS in each scenario. The better performance of the DE and GAs is because of the fact that DE and GAs are population-based meta-heuristics, while PS is a single-solution-based algorithm, while comparison shows DE is relatively better than GAs. Robustness of the design schemes is established through estimation power signal parameters with different SNRs (70 db, 30 db and no noise), and results show that with the increase in noise variance, the accuracy of DE, GAs and PS algorithms degrades, yet the performance of both DE and GAs is found still reasonable in precision. Statistical results based on mean and STD values of MAE, RMSE and ER^2 performance indices along with their global versions as well as illustrations of histograms, cumulative distribution functions and stacked bar validate the consistent accuracy of DE and GAs in each case. The superior performance of DE is further endorsed through ANOVA-based statistical test. Complexity analyses for all three algorithms show that by increasing the optimization variables in the signal model the complexity of the algorithms increases, while the gauges of complexity operators are greater for GAs than the rest. One may explore recently introduced variants of modern optimization procedures for the better performance such as firefly algorithm, backtracking search algorithm, fractional particle swarm optimization, fireworks and gravitational search algorithm.

Table 11 Magnitudes of global performance metrics for each variation of the first five examples of power signal model

Method	Example	Noise (db)	$\bar{\varepsilon}$		G_{MAE}		G_{RMSE}		G_{ER^2}	
			Mean	STD	Mean	STD	Mean	STD	Mean	STD
DE	1	0	7.30E−21	4.79E−21	6.04E−11	1.80E−11	6.94E−11	1.96E−11	5.19E−18	1.65E−18
		70	5.92E−08	1.09E−16	1.57E−05	2.48E−10	1.76E−05	3.56E−10	6.16E−11	2.49E−15
		30	6.44E−04	1.49E−15	7.72E−04	2.23E−11	8.63E−04	1.86E−11	1.48E−07	6.38E−15
	2	0	4.48E−02	7.32E−02	3.75E−01	5.62E−01	5.29E−01	1.23E−00	7.34E−00	6.40E−01
		70	4.17E−02	7.15E−02	5.28E−01	1.05E−00	9.16E−01	2.47E−00	2.84E−01	1.33E−02
		30	4.17E−02	6.52E−02	3.81E−01	5.58E−01	5.32E−01	1.23E−00	7.34E−00	6.39E−01
	3	0	1.26E−18	1.57E−18	7.34E−10	3.94E−10	8.85E−10	4.74E−10	1.11E−18	1.11E−17
		70	5.97E−08	1.34E−15	5.91E−06	2.87E−09	8.21E−06	5.39E−09	3.28E−10	4.30E−13
		30	6.33E−04	8.04E−15	1.02E−03	2.32E−09	1.18E−03	3.29E−09	6.79E−06	3.77E−11
	4	0	2.44E−02	5.63E−02	2.33E−00	2.00E−01	5.51E−00	4.89E−01	9.62E−03	9.62E−04
		70	2.71E−02	5.94E−02	4.58E−01	3.23E−02	1.12E−02	7.91E−02	2.53E−06	1.84E−07
		30	1.75E−02	4.55E−02	2.38E−01	2.11E−02	5.80E−01	5.16E−02	1.07E−06	1.06E−07
	5	0	4.95E−02	9.33E−02	6.21E−01	4.63E−02	1.85E−02	1.39E−03	8.10E−06	7.59E−07
		70	5.19E−02	9.78E−02	7.05E−01	5.09E−02	2.10E−02	1.53E−03	9.77E−06	9.39E−07
		30	3.21E−02	7.50E−02	3.12E−02	1.48E−03	9.35E−02	4.43E−03	8.46E−07	6.05E−08
GA	1	0	8.15E−16	2.23E−16	2.04E−08	3.79E−09	2.38E−08	3.88E−09	1.55E−16	1.02E−16
		70	5.92E−08	1.59E−14	1.57E−05	1.69E−08	1.76E−05	2.82E−08	6.16E−11	1.98E−13
		30	6.44E−04	6.10E−11	7.72E−04	1.11E−06	8.63E−04	9.98E−07	1.48E−07	3.43E−10
	2	0	2.02E−03	8.29E−03	1.93E−01	1.37E−01	2.30E−01	1.60E−01	3.22E−01	2.50E−01
		70	3.04E−03	1.15E−02	1.79E−01	1.40E−01	2.15E−01	1.64E−01	3.00E−01	2.53E−01
		30	5.27E−03	1.41E−02	1.87E−01	1.43E−01	2.24E−01	1.68E−01	3.21E−01	3.01E−01
	3	0	7.59E−15	1.74E−14	4.65E−08	3.84E−08	5.79E−08	5.12E−08	2.89E−14	6.72E−14
		70	6.33E−08	8.84E−14	1.23E−05	2.28E−07	1.54E−05	2.54E−07	1.15E−09	3.80E−11
		30	6.28E−04	1.98E−10	7.73E−04	8.37E−06	9.49E−04	6.93E−06	4.38E−06	6.36E−08
	4	0	2.80E−03	1.02E−02	2.40E−02	3.28E−02	3.36E−02	4.52E−02	1.26E−02	1.96E−02
		70	2.33E−03	6.83E−03	2.41E−02	4.32E−02	3.44E−02	6.50E−02	2.15E−02	1.08E−01
		30	3.00E−03	1.01E−02	1.76E−02	2.99E−02	2.45E−02	4.09E−02	9.04E−03	1.81E−02
	5	0	7.75E−03	1.94E−02	2.02E−01	8.54E−02	2.66E−01	1.08E−01	3.43E−01	2.46E−01
		70	9.13E−03	2.04E−02	2.07E−01	8.65E−02	2.76E−01	1.17E−01	3.72E−01	2.83E−01
		30	6.40E−03	1.70E−02	1.80E−01	9.96E−02	2.35E−01	1.26E−01	2.96E−01	2.45E−01
PS	1	0	8.48E−31	1.41E−45	5.00E−16	0.00E−00	7.45E−16	2.97E−31	0.00E−00	0.00E−00
		70	5.92E−08	8.65E−23	1.58E−05	0.00E−00	1.79E−05	3.06E−20	6.34E−11	0.00E−00
		30	6.44E−04	1.42E−18	8.11E−04	0.00E−00	9.00E−04	8.72E−19	1.61E−07	0.00E−00
	2	0	2.55E−01	1.98E−01	4.72E−01	2.27E−01	5.76E−01	2.48E−01	1.62E−00	1.17E−00
		70	3.07E−01	1.83E−01	4.99E−01	2.17E−01	6.10E−01	2.29E−01	1.74E−00	1.24E−00
		30	2.84E−01	1.82E−01	4.85E−01	2.08E−01	5.94E−01	2.30E−01	1.67E−00	1.17E−00
	3	0	1.42E−30	6.48E−31	9.25E−16	2.63E−16	1.07E−15	2.56E−16	0.00E−00	0.00E−00
		70	6.60E−08	1.41E−14	1.72E−05	3.93E−08	2.13E−05	5.77E−08	2.21E−09	1.20E−11
		30	6.07E−04	7.58E−11	3.29E−04	3.49E−06	4.03E−04	3.21E−06	7.91E−07	1.26E−08
	4	0	7.01E−01	3.09E−01	6.51E−01	3.05E−01	7.70E−01	3.22E−01	2.79E−00	1.91E−00
		70	6.91E−01	3.24E−01	6.81E−01	2.96E−01	7.79E−01	2.97E−01	2.78E−00	1.76E−00
		30	6.27E−01	3.21E−01	6.56E−01	3.10E−01	7.79E−01	3.04E−01	2.80E−00	1.83E−00
	5	0	3.31E−01	1.90E−01	4.94E−01	1.82E−01	5.89E−01	1.89E−01	1.59E−00	8.96E−01
		70	3.30E−01	1.89E−01	5.19E−01	1.64E−01	6.28E−01	1.66E−01	1.76E−00	8.77E−01
		30	3.47E−01	1.84E−01	5.35E−01	1.96E−01	6.40E−01	2.01E−01	1.87E−00	1.11E−00

Table 12 Results of ANOVA test for example 4 of power signal model with 70-dB SNR

Scheme	Method Null hypothesis All means are equal Alternative hypothesis At least one mean is different Significance level α = 0.05 Equal variances were assumed for the analysis.
DE	**Analysis of Variance** Source D F-Value P-Value Factor 2 0.11 0.895 Error 87 Total 89 **Model Summary** R-sq 0.25% **Means** Factor N Mean StDev 95% CI C1 30 0.000772 0.000000 (0.000772, 0.000772) C2 30 0.000772 0.000000 (0.000772, 0.000772) C3 30 0.000772 0.000000 (0.000772, 0.000772) Pooled StDev = 2.330566E-11
GA	**Analysis of Variance** Source DF F-Value P-Value Factor 2 0.21 0.810 Error 90 Total 92 **Model Summary** R-sq 0.47% **Means**
	Factor N Mean StDev 95% CI C1 31 0.000772 0.000002 (0.000772, 0.000773) C2 31 0.000772 0.000001 (0.000772, 0.000772) C3 31 0.000772 0.000001 (0.000772, 0.000772) Pooled StDev = 1.156001E-06
PS	**Analysis of Variance** Source DF F-Value P-Value Factor 2 0.20 0.821 Error 87 Total 89 **Model Summary** S R-sq R-sq(adj) R-sq(pred) 0.0311486 0.45% 0.00% 0.00% **Means** Factor N Mean StDev 95% CI C1 30 0.02335 0.03230 (0.01205, 0.03466) C2 30 0.01830 0.02975 (0.00700, 0.02960) C3 30 0.02086 0.03135 (0.00956, 0.03216) Pooled StDev = 0.0311486

Table 13 Results of ANOVA test for example 5 of power signal model with 30-dB SNR

Scheme	Method Null hypothesis All means are equal Alternative hypothesis At least one mean is different Significance level α = 0.05 Equal variances were assumed for the analysis.
DE	**Analysis of Variance** Source DF F-Value P-Value Factor 2 0.11 0.897 Error 87 Total 89 **Model Summary** R-sq 0.25% **Means** Factor N Mean StDev 95% CI C1 30 0.000774 0.000007 (0.000770, 0.000777) C2 30 0.000773 0.000010 (0.000770, 0.000777) C3 30 0.000773 0.000010 (0.000769, 0.000776) Pooled StDev = 8.837867E-06
GA	**Analysis of Variance** Source DF F-Value P-Value Factor 2 0.36 0.695 Error 87 Total 89 **Model Summary** R-sq
	0.83% **Means** Factor N Mean StDev 95% CI C1 30 0.01630 0.02818 (0.00600, 0.02660) C2 30 0.02064 0.03039 (0.01034, 0.03094) C3 30 0.01456 0.02646 (0.00426, 0.02487) Pooled StDev = 0.0283875
PS	**Analysis of Variance** Source DF F-Value P-Value Factor 2 2.29 0.107 Error 87 Total 89 **Model Summary** R-sq 5.00% **Means** Factor N Mean StDev 95% CI C1 30 0.1561 0.1331 (0.1044, 0.2079) C2 30 0.2286 0.1330 (0.1768, 0.2803) C3 30 0.1655 0.1600 (0.1138, 0.2173) Pooled StDev = 0.14258

Table 14 Comparison of computational complexity comparison for each SNR level of the first five power signal model examples

Method	Example	Noise (dB)	Complexity operators					
			Time		Generations		Function counts	
			Mean	STD	Mean	STD	Mean	STD
DE	1	0	00.75	0.08	111.44	2.18	13,351.37	1373.66
		70	00.80	0.02	118.21	2.92	14,302.41	353.00
		30	00.97	0.03	142.79	4.10	17,276.59	496.16
	2	0	17.70	6.60	325.13	116.68	58,847.53	21,118.65
		70	18.53	6.62	326.09	115.03	59,021.29	20,820.83
		30	19.25	5.80	337.90	96.94	61,158.90	17,546.86
	3	0	07.74	0.27	130.84	2.62	23,681.04	474.17
		70	07.55	0.18	128.98	2.67	23,344.38	484.02
		30	09.60	0.28	163.50	4.37	29,592.50	791.47
	4	0	18.25	6.12	281.47	89.55	50,945.07	16,207.65
		70	19.26	6.40	263.36	83.35	47,667.16	15,085.65
		30	18.92	5.86	308.21	93.53	55,785.01	16,929.27
	5	0	23.62	10.67	316.06	143.69	85,651.26	38,940.00
		70	25.47	11.84	324.96	150.66	88,063.16	40,827.56
		30	30.87	13.26	408.38	189.67	110,669.98	51,401.32
GA	1	0	34.67	3.46	500.00	0.00	120,240.00	0000.0
		70	38.78	3.48	500.00	0.00	120,240.00	0000.0
		30	34.49	6.09	500.00	0.00	120,240.00	0000.0
	2	0	35.48	6.73	500.00	0.00	120,240.00	0000.0
		70	36.14	5.93	500.00	0.00	120,240.00	0000.0
		30	31.11	1.24	500.00	0.00	120,240.00	0000.0
	3	0	34.26	1.52	500.00	0.00	120,240.00	0000.0
		70	36.32	4.89	500.00	0.00	120,240.00	0000.0
		30	35.47	4.08	500.00	0.00	120,240.00	0000.0
	4	0	39.12	3.46	500.00	0.00	120,240.00	0000.0
		70	41.34	3.48	500.00	0.00	120,240.00	0000.0
		30	38.45	6.09	500.00	0.00	120,240.00	0000.0
	5	0	37.76	6.73	500.00	0.00	120,240.00	0000.0
		70	39.87	5.93	500.00	0.00	120,240.00	0000.0
		30	42.88	1.24	500.00	0.00	120,240.00	0000.0
PS	1	0	0.08	0.22	0158.00	034.00	01,040.00	2166.00
		70	0.10	0.27	0186.00	075.00	01,229.00	2965.00
		30	0.15	0.26	0290.00	174.00	01,977.00	2854.00
	2	0	3.12	1.17	1003.94	366.09	08,695.92	3127.59
		70	3.16	1.25	1012.86	386.10	08,742.43	3272.93
		30	3.56	1.35	0989.53	353.90	08,559.28	3055.10
	3	0	1.20	0.20	0372.34	021.18	03,648.10	0424.28
		70	1.51	0.35	0478.67	111.88	04,673.17	1072.65
		30	1.28	0.25	0401.00	077.74	03,928.17	0677.39
	4	0	3.59	0.96	1192.45	318.82	10,351.67	2749.62
		70	3.51	1.23	1139.74	331.37	09,827.48	3084.19
		30	3.25	1.11	1131.66	342.60	09,617.03	3195.08
	5	0	1.63	0.10	0501.00	000.00	05,757.49	0285.24
		70	1.62	0.09	0501.00	000.00	05,749.90	0240.40
		30	1.65	0.10	0501.00	000.00	05,757.46	0279.67

It seems to be a potential research direction to study other metaheuristics based on the swarming optimization, fractional evolutionary PSO, scatter search and backtracking search optimization algorithm for power signals parameter estimation.

Compliance with ethical standards

Conflict of interest All authors declare that there is no conflict of interest.

References

1. Rashid MH (2010) Power electronics handbook: devices, circuits and applications. Academic press, Cambridge
2. Erickson RW, Maksimovic D (2007) Fundamentals of power electronics. Springer, Berlin
3. Ray PK, Puhan PS, Panda G (2016) Real time harmonics estimation of distorted power system signal. Int J Electr Power Energy Syst 75:91–98
4. Hamidi RJ, Livani H (2018) Adaptive single-phase auto-reclosing method using power line carrier signals. Int J Electr Power Energy Syst 96:64–73
5. Singh SK, Sinha N, Goswami AK, Sinha N (2016) Several variants of Kalman Filter algorithm for power system harmonic estimation. Int J Electr Power Energy Syst 78:793–800
6. Dwivedi UD, Shakya D, Singh SN (2008) Power quality monitoring and analysis: an overview and key issues. Int J Syst Signal Control Eng Appl 1(1):74–88
7. Qian H, Zhao R, Chen T (2007) Interharmonics analysis based on interpolating windowed FFT algorithm. IEEE Trans Power Deliv 22(2):1064–1069
8. Bian J, Xing J, Liu J, Li Z, Li H (2016) An adaptive and computationally efficient algorithm for parameters estimation of superimposed exponential signals with observations missing randomly. Digit Signal Proc 48:148–162
9. Bai ZD, Rao CR, Wu YH, Zen MM, Zhao LC (1999) The simultaneous estimation of the number of signals and frequencies of multiple sinusoids when some observations are missing: I. Asymptotics. Proc Natl Acad Sci USA 96(11):106–111
10. Cao Y, Liu Z (2010) Signal frequency and parameter estimation for power systems using the hierarchical identification principle. Math Comput Model 52(5):854–861
11. Xu L, Ding F (2017) Recursive least squares and multi-innovation stochastic gradient parameter estimation methods for signal modeling. Circuits Syst Signal Process 36(4):1735–1753
12. Zubair S, Chaudhary NI, Khan ZA, Wang W (2018) Momentum fractional LMS for power signal parameter estimation. Sig Process 142:441–449
13. Barkat B (2018) A quadratic model for the far-field direction of arrival estimation. Digit Signal Proc 72:208–215
14. Singh SK, Goswami AK, Sinha N (2015) Power system harmonic parameter estimation using Bilinear Recursive Least Square (BRLS) algorithm. Int J Electr Power Energy Syst 67:1–10
15. Badoni M, Singh A, Singh B (2015) Variable forgetting factor recursive least square control algorithm for DSTATCOM. IEEE Trans Power Deliv 30(5):2353–2361
16. Singh SK, Sinha N, Goswami AK, Sinha N (2015) Variable Constraint based Least Mean Square algorithm for power system harmonic parameter estimation. Int J Electr Power Energy Syst 73:218–228
17. Veček N, Črepinšek M, Mernik M (2017) On the influence of the number of algorithms, problems, and independent runs in the comparison of evolutionary algorithms. Appl Soft Comput 54:23–45
18. Ravber M, Mernik M, Črepinšek M (2017) The impact of quality indicators on the rating of multi-objective evolutionary algorithms. Appl Soft Comput 55:265–275
19. Jesenko D, Mernik M, Žalik B, Mongus D (2017) Two-level evolutionary algorithm for discovering relations between nodes' features in a complex network. Appl Soft Comput 56:82–93
20. He C, Tian Y, Jin Y, Zhang X, Pan L (2017) A radial space division based evolutionary algorithm for many-objective optimization. Appl Soft Comput 61:603–621
21. Masood Z et al (2017) Design of Mexican Hat Wavelet neural networks for solving Bratu type nonlinear systems. Neurocomputing 221:1–14
22. Raja MAZ, Farooq U, Chaudhary NI, Wazwaz AM (2016) Stochastic numerical solver for nanofluidic problems containing multi-walled carbon nanotubes. Appl Soft Comput 38:561–586
23. Raja MAZ, Mehmood A, Niazi SA, Shah SM Computational intelligence methodology for the analysis of RC circuit modelled with nonlinear differential order system. Neural Comput Appl 1–20
24. Raja MAZ (2014) Solution of the one-dimensional Bratu equation arising in the fuel ignition model using ANN optimised with PSO and SQP. Connect Sci 26(3):195–214
25. Heidari AA, Abbaspour RA, Jordehi AR (2017) Gaussian barebones water cycle algorithm for optimal reactive power dispatch in electrical power systems. Appl Soft Comput 57:657–671
26. El-Fergany AA, Hasanien HM (2018) Tree-seed algorithm for solving optimal power flow problem in large-scale power systems incorporating validations and comparisons. Appl Soft Comput 64:307–316
27. Raja MAZ, Shah AA, Mehmood A, Chaudhary NI, Aslam MS (2018) Bio-inspired computational heuristics for parameter estimation of nonlinear Hammerstein controlled autoregressive system. Neural Comput Appl 29(12):1455–1474
28. Raja MAZ, Shah FH, Alaidarous ES, Syam MI (2017) Design of bio-inspired heuristic technique integrated with interior-point algorithm to analyze the dynamics of heartbeat model. Appl Soft Comput 52:605–629
29. Raja MAZ, Aslam MS, Chaudhary NI, Nawaz M, Shah SM Design of hybrid nature-inspired heuristics with application to active noise control systems. Neural Comput Appl pp 1–29
30. Hitomi N, Selva D (2018) Incorporating expert knowledge into evolutionary algorithms with operators and constraints to design satellite systems. Appl Soft Comput 66:330–345
31. Raja MAZ, Ahmed T, Shah SM (2017) Intelligent computing strategy to analyze the dynamics of convective heat transfer in MHD slip flow over stretching surface involving carbon nanotubes. J Taiwan Inst Chem Eng 80:935–953
32. Raja MAZ, Niazi SA, Butt SA (2017) An intelligent computing technique to analyze the vibrational dynamics of rotating electrical machine. Neurocomputing 219:280–299. https://doi.org/10.1016/j.neucom.2016.09.032
33. Zameer A et al (2017) Intelligent and robust prediction of short term wind power using genetic programming based ensemble of neural networks. Energy Convers Manag 134:361–372
34. Majeed K, Masood Z, Samar R, Raja MAZ (2017) A genetic algorithm optimized Morlet wavelet artificial neural network to study the dynamics of nonlinear Troesch's system. Appl Soft Comput 56:420–435

35. Ahmad I et al (2016) Bio-inspired computational heuristics to study Lane–Emden systems arising in astrophysics model. SpringerPlus 5(1):1866
36. Raja MAZ, Zameer A, Khan AU, Wazwaz AM (2016) A new numerical approach to solve Thomas–Fermi model of an atom using bio-inspired heuristics integrated with sequential quadratic Programming. SpringerPlus 5(1):1400
37. Akbar S et al (2017) Design of bio-inspired heuristic techniques hybridized with sequential quadratic programming for joint parameters estimation of electromagnetic plane waves. Wireless Pers Commun 96(1):1475–1494
38. Naderi E, Azizivahed A, Narimani H, Fathi M, Narimani MR (2017) A comprehensive study of practical economic dispatch problems by a new hybrid evolutionary algorithm. Appl Soft Comput 61:1186–1206
39. Ara A et al (2018) Wavelets optimization method for evaluation of fractional partial differential equations: an application to financial modelling. Adv Differ Equ 2018(1):8
40. Li X, Ding F (2013) Signal modeling using the gradient search. Appl Math Lett 26(8):807–813
41. Zhou L, Li X, Xu H, Zhu P (2016) Multi-innovation stochastic gradient method for harmonic modelling of power signals. IET Signal Proc 10(7):737–742
42. Chaudhary NI, Zubair S, Raja MAZ (2017) A new computing approach for power signal modeling using fractional adaptive algorithms. ISA Trans 68:189–202
43. Storn R, Price K (1997) Differential evolution—a simple and efficient heuristic for global optimization over continuous spaces. J Glob Optim 11(4):341–359
44. Diab DM, El Hindi KM (2017) Using differential evolution for fine tuning naïve Bayesian classifiers and its application for text classification. Appl Soft Comput 54:183–199
45. Sakr WS, El-Sehiemy RA, Azmy AM (2017) Adaptive differential evolution algorithm for efficient reactive power management. Appl Soft Comput 53:336–351
46. Feng ZK, Niu WJ, Zhou JZ, Cheng CT, Zhang YC (2017) Scheduling of short-term hydrothermal energy system by parallel multi-objective differential evolution. Appl Soft Comput 61:58–71
47. Rajesh K, Kannan S, Thangaraj C (2016) Least cost generation expansion planning with wind power plant incorporating emission using differential evolution algorithm. Int J Electr Power Energy Syst 80:275–286
48. Fateh MF et al (2017) Biologically inspired computing framework for solving two-point boundary value problems using differential evolution. Neural Comput Appl 28(8):2165–2179
49. Ara A et al (2018) Numerical simulation for Jeffery–Hamel flow and heat transfer of micropolar fluid based on differential evolution algorithm. AIP Adv 8(1):015201
50. Das S, Mullick SS, Suganthan PN (2016) Recent advances in differential evolution—an updated survey. Swarm Evolut Comput 27:1–30
51. Piotrowski AP (2017) Review of differential evolution population size. Swarm Evolut Comput 32:1–24
52. Jebaraj L, Venkatesan C, Soubache I, Rajan CCA (2017) Application of differential evolution algorithm in static and dynamic economic or emission dispatch problem: a review. Renew Sustain Energy Rev 77:1206–1220
53. Das S, Suganthan PN (2011) Differential evolution: a survey of the state-of-the-art. IEEE Trans Evol Comput 15(1):4–31
54. Mitchell M (1998) An introduction to genetic algorithms. MIT Press, Cambridge
55. Coley DA (1999) An introduction to genetic algorithms for scientists and engineers. World Scientific Publishing Company
56. Fernández RÁ, Caraballo SC, Cilleruelo FB, Lozano JA (2018) Fuel optimization strategy for hydrogen fuel cell range extender vehicles applying genetic algorithms. Renew Sustain Energy Rev 81:655–668
57. Mehmood A et al (2018) Intelligent computing to analyze the dynamics of Magnetohydrodynamic flow over stretchable rotating disk model. Appl Soft Comput 67:8–28
58. Horton P, Jaboyedoff M, Obled C (2018) Using genetic algorithms to optimize the analogue method for precipitation prediction in the Swiss Alps. J Hydrol 556:1220–1231
59. Raja MAZ, Aslam MS, Chaudhary NI, Khan WU (2018) Bio-inspired heuristics hybrid with interior-point method for active noise control systems without identification of secondary path. Front Inf Technol Electron Eng 19(2):246–259
60. Oztekin A, Al-Ebbini L, Sevkli Z, Delen D (2018) A decision analytic approach to predicting quality of life for lung transplant recipients: a hybrid genetic algorithms-based methodology. Eur J Oper Res 266(2):639–651
61. Raja MAZ, Zameer A, Kiani AK, Shehzad A, Khan MAR (2018) Nature-inspired computational intelligence integration with Nelder–Mead method to solve nonlinear benchmark models. Neural Comput Appl 29(4):1169–1193
62. Hooke R, Jeeves TA (1961) Direct search solution of numerical and statistical problems. J ACM (JACM) 8(2):212–229
63. Chouhdry ZR, Hasan KM, Raja MAZ (2018) Design of reduced search space strategy based on integration of Nelder–Mead method and pattern search algorithm with application to economic load dispatch problem. Neural Comput Appl 30:3693–3705. https://doi.org/10.1007/s00521-017-2951-6
64. Kumar LS, Kumar GN, Madichetty S (2017) Pattern search algorithm based automatic online parameter estimation for AGC with effects of wind power. Int J Electr Power Energy Syst 84:135–142
65. Narang N, Sharma E, Dhillon JS (2017) Combined heat and power economic dispatch using integrated civilized swarm optimization and Powell's pattern search method. Appl Soft Comput 52:190–202
66. Guo N, Yang Z, Wang L, Ouyang Y, Zhang X (2018) Dynamic model updating based on strain mode shape and natural frequency using hybrid pattern search technique. J Sound Vib 422:112–130